Kinetic control of stationary flux ratios for a wide range of biochemical processes

Joel D. Mallory[†], Anatoly B. Kolomeisky[*,†,‡,§,‖], and Oleg A. Igoshin[*,†,‡,⊥]
[†] *Center for Theoretical Biological Physics, Rice University, Houston TX 77005*
[‡] *Department of Chemistry, Rice University, Houston, TX 77005*
[§] *Department of Chemical and Biomolecular Engineering, Rice University, Houston, TX 77005*
[‖] *Department of Physics and Astronomy, Rice University, Houston, TX 77005 and*
[⊥] *Department of Bioengineering and of Biosciences, Rice University, Houston, TX 77005*
(Dated: November 27, 2019)

ABSTRACT

One of the most intriguing features of biological systems is their ability to regulate the steady-state fluxes of the underlying biochemical reactions, however the regulatory mechanisms and their physicochemical properties are not fully understood. Fundamentally, flux regulation can be explained with a chemical kinetic formalism describing the transitions between discrete states with the reaction rates defined by an underlying free-energy landscape. Which features of the energy landscape affect the flux distribution? Here we prove that the ratios of the steady-state fluxes are invariant to energy perturbations of the discrete states and are only affected by the energy barriers. In other words, the non-equilibrium flux distribution is under kinetic and not thermodynamic control. We illustrate the generality of this result for three biological processes. For the network describing protein folding along competing pathways, the probabilities of proceeding via these pathways are shown to be invariant to the stability of the intermediates or to the presence of additional misfolded states. For the network describing protein synthesis, the error rate and the energy expenditure per peptide bond is proven to be independent of the stability of the intermediate states. For molecular motors such as myosin-V, the ratio of forward to backward steps and the number of ATP molecules hydrolyzed per step is demonstrated to be invariant to energy perturbations of the intermediate states. These findings place important constraints on the ability of mutations and drug perturbations to affect the steady-state flux distribution for a wide class of biological processes.

INTRODUCTION

Chemical kinetics represents a fundamental mesoscopic formalism to understand many biological phenomena with a wide range of major cellular processes described in terms of the complex networks of biochemical reactions[1]. When the mechanistic details of the process are known, the underlying mechanisms can be represented as elementary steps described by mass-action kinetics of first order reactions (e.g., for catalysis, conformational transitions, and dissociation) or second order reactions for bimolecular binding transitions. This formalism allows one to study the kinetics of enzymatically controlled reactions and resulting kinetic laws[2], transformations between different states of promoters and resulting transcription rates[3–6], transitions between receptor-complexes and resulting signaling[7,8], and many other phenomena[9,10]. In many of these examples, the time-scale of changes in the concentrations of unbound molecular species is much slower than the time-scale of transitions between the states of the macromolecular systems. For example, concentrations of substrates and products of enzymatic catalysis change much slower than transitions between the different enzyme states[11]. In this regime, second-order binding reactions can be approximated effectively as first-order transitions resulting in the so-called linear framework[12]. In that framework, many biologically important system properties can be expressed in terms of steady-state probabilities and fluxes of the resulting effective first-order reaction networks.

Fundamentally, the kinetics of elementary chemical transitions can be understood in terms of the underlying free-energy landscape with the rate of each step affected by the difference between the energy of the state and the barriers separating reactants from products[13]. For reaction networks with cycles that do not change the concentrations of the molecular species in the cellular environment, the underlying chemical reaction rates are subject to the detailed balance constraints[14]. In that case, the resulting steady-state probabilities are computed from the Boltzmann distribution, and they only depend on the free energy of the states that are independent of the free energy barriers[14]. In contrast to the kinetic control regime when the barrier heights determine the resulting distributions, this regime is often referred to as thermodynamic control[15]. For example, models of binding and dissociation of transcription factors to DNA and resulting transcription rates in bacteria are often calculated in the equilibrium thermodynamics framework[16,17].

But in many other biologically relevant cases, transitions between states of the macro-molecular system are coupled with the changes in the pool of cellular cofactor molecules. For example, transitions between states of enzymes and molecular motors can be coupled to the hydrolysis of ATP[18,19]. In that case, the system reaches a non-equilibrium steady-state, where the steady-state probabilities and the fluxes depend on the energies of the transition states. Thus, non-equilibrium steady-states may be under a combination of thermodynamic and ki-

netic controls, and it is not clear which features of the free energy landscape control key system properties.

In non-equilibrium conditions, the stationary fluxes between the states can approach non-zero values with important biological implications. For example, the rate of an enzymatic reaction, the speed of a molecular motor, and many other crucial characteristics are proportional to these steady-state fluxes[14,20]. Moreover, many important properties can be related to the ratios of the steady-state fluxes. Specifically, the enzyme selectivity or the error rate that quantifies the ability of enzymes to discriminate between right (cognate) and wrong (non-cognate) substrates can be expressed as the ratio of the catalytic fluxes to the corresponding states[18,21,22]. In the same way, the efficiency of a molecular motor can be expressed in terms of the ratio of forward-stepping and futile cycle fluxes[20,23]. Notably, our previous research[24] has shown that for both Michaelis-Menten (MM) and the Hopfield kinetic proofreading (KPR) mechanism[18], the error rate is purely under kinetic control. As such, the error rate is only a function of the differences in the free energy barriers for pathways leading to the right and wrong substrates, and it is independent of the differences of the stabilities of the corresponding states. Here we aim to generalize this result to other properties of biological systems.

In this work, we use a chemical kinetic formalism to determine how steady-state probabilities and flux distribution of the underlying biochemical reactions are affected by perturbations of the underlying free energy landscape. The results allow us to prove that an arbitrary ratio of the steady-state fluxes is invariant to the energy perturbations of the stabilities of the discrete states, and therefore, is only dependent on the free energy barriers. In other words, we demonstrate that the corresponding biological properties that are expressed in terms of the steady-state flux ratios are governed by kinetic and not by thermodynamic factors. We illustrate the generality and the biological implications of our results by specifically studying three diverse biological systems. The examples include: (i) two alternative pathways for protein folding in the presence of misfolded error states, which is motivated by folding pathways in hen egg-white lysozyme[25,26], (ii) a Hopfield KPR network describing aminoacyl(aa)-tRNA selection during protein translation in the *Escherichia coli* ribosome[18,24,27–30], and (iii) the myosin-V motor protein that walks along actin cytoskeleton filaments[20,23]. These results have wide-ranging implications for the types of genetic or chemical perturbations capable of changing the steady-state flux distribution through biochemical reaction networks.

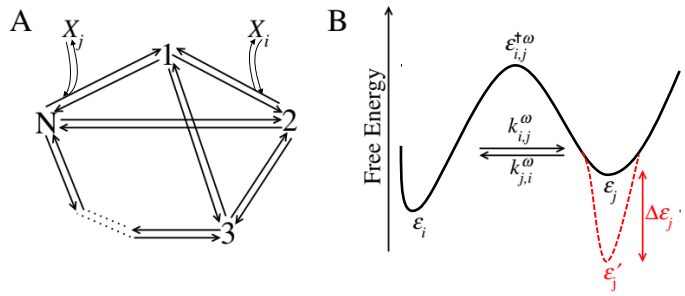

FIG. 1. Representation of a general biochemical kinetic network and a portion of its free energy landscape. (A) General biochemical network comprised of N different states. The various internal states of the system are denoted by the numbers $1, .., N$, while the cofactor molecules in the bath that are involved in the various bimolecular reactions have chemical identities denoted by X_i and X_j, respectively. (B) A portion of a free energy landscape corresponding to the reaction between the states i and j with the energies of the respective intermediate states (well-depths) denoted by ϵ_i and ϵ_j and the transition state energy denoted by $\epsilon_{i,j}^{\dagger\omega}$. The respective rate constants $k_{i,j}^{\omega}$ and $k_{j,i}^{\omega}$ correspond to the forward and reverse reactions between the two states i and j on the pathway ω. Note that the energy of the state j is decreased (perturbed) by an amount $\Delta\epsilon_j$ (red, dashed curve) such that the energy of the perturbed state is $\epsilon_j' = \epsilon_j - \Delta\epsilon_j$.

METHODS

Notation and Setup

Consider an arbitrary biochemical system described by the linear formalism[12], i.e., by a chemical kinetic network with quasi-first order transitions between N biochemical states (see Fig. 1A) with the rate constant for a reaction $i \to j$ (i.e., a transition from the i-th state to the j-th state) denoted as $k_{i,j}$. Generally, there could be multiple elementary reactions between the states i and j. Therefore,

$$k_{i,j} = \sum_{\omega} k_{i,j}^{\omega}, \tag{1}$$

where the index ω runs over all of the possible reaction pathways $i \to j$. Note also that for each reaction the rate constants $k_{i,j}^{\omega}$ can be expressed in a generalized Kramer's form:

$$k_{i,j}^{\omega} = k_{i,j}^{0\omega} e^{\epsilon_i - \epsilon_{i,j}^{\dagger\omega}}, \tag{2}$$

in which the prefactors of the biomolecular reactions that were initially second order (i.e., with cofactor binding steps) included the dependence on the chemical potentials μ_γ of the these cofactors (see SI for discussion). Here ϵ_i and $\epsilon_{i,j}^{\dagger\omega}$ are respectively energies of the i-th state and the barrier heights (transitions state energies) for a given reaction in units of $k_B T$ (see Fig. 1B).

In the limit of $t \to \infty$, the system is characterized by a stationary probability distribution vector with N

components, $\mathbf{P} = [P_1, P_2..., P_N]^T$ that can be obtained by solving a set of steady-state forward master equations subject to the normalization condition:

$$\mathbf{K} \cdot \mathbf{P} = \mathbf{0} \text{ and } \mathbf{1}^T \cdot \mathbf{P} = 1, \tag{3}$$

where $\mathbf{1}$ is $N \times 1$ unit vector, and the $\mathbf{K}$ is an $N \times N$ rate matrix:

$$K_{j,i} = \begin{cases} k_{i,j}, & \text{for } j \neq i \\ -\sum_{i \neq j} k_{i,j}, & \text{for } j = i. \end{cases} \tag{4}$$

Assuming this matrix is not rank deficient, (3) has a unique solution for the stationary probability distribution $\mathbf{P}$. The corresponding steady-state fluxes $J^{\omega}_{i,j}$ for the transition $i \to j$ are given by

$$J^{\omega}_{i,j} = k^{\omega}_{i,j} P_i. \tag{5}$$

Depending on whether the rate constants $k^{0\omega}_{i,j}$ are subject to the detailed balance constraints, this formalism can describe both equilibrium and non-equilibrium steady states. In the former case, the fluxes balance $J^{\omega}_{i,j} = J^{\omega}_{j,i}$ and the stationary probability distribution corresponds to the Boltzmann distribution, i.e., it can be expressed in terms of the energies of the individual states ϵ_i ($P_i = e^{-\epsilon_i}/Z$) and is independent of the barrier heights $\epsilon^{\dagger\omega}_{i,j}$[14]. Below we explore how non-equilibrium steady-state fluxes and the probabilities depend on these energies.

Perturbation of the Free Energy Landscape

Consider a perturbation that decreases the energy of an arbitrary state m on the free-energy landscape of the system by an amount $\Delta\epsilon_m$, i.e., such that its energy changes to $\epsilon'_m = \epsilon_m - \Delta\epsilon_m$ (see Fig. 1*B*). Here and below the prime symbol $'$ denotes the parameters following this perturbation. Assume that the energies of other states, namely, the transition state energies $\epsilon^{\dagger\omega}_{i,j}$ and the chemical potentials μ_γ [see SI Eqs. (S8-S10)] of all of the cofactor molecules in the bath are held constant.

From (2), the perturbation reduces all of the rate constants for the reactions $m \to j$ by a factor of $e^{-\Delta\epsilon_m}$, but all of the other rate constants $k^{\omega}_{i,j}$ remain the same:

$$k'^{\omega}_{i,j} = \begin{cases} k^{\omega}_{i,j}, & \text{for } i \neq m \\ k^{\omega}_{m,j} e^{-\Delta\epsilon_m}, & \text{for } i = m. \end{cases} \tag{6}$$

The perturbed steady-state probability distribution $\mathbf{P'}$ satisfies equations of the form of (3) with the perturbed matrix $\mathbf{K'}$:

$$K'_{j,i} = \begin{cases} K_{j,i}, & \text{for } i \neq m \\ K_{j,m} e^{-\Delta\epsilon_m}, & \text{for } i = m, \end{cases} \tag{7}$$

i.e., with the entire m-th column scaled by a factor of $e^{-\Delta\epsilon_m}$. It is not hard to show [see the SI Eq. (S15)] that perturbed probabilities P'_i can be expressed in terms of unperturbed probabilities P_i as follows

$$P'_i = \begin{cases} \alpha P_i, & \text{for } i \neq m \\ \alpha P_m e^{\Delta\epsilon_m}, & \text{for } i = m. \end{cases} \tag{8}$$

Here α is a normalization constant,

$$\alpha = \frac{1}{\sum_{j \neq m} P_j + P_m e^{\Delta\epsilon_m}}, \tag{9}$$

that guarantees the conservation of probability, $\mathbf{1}^T \cdot \mathbf{P'} = 1$.

Invariance of the Ratios of the Steady-State Fluxes

Using (6) and (8) in (5), we conclude that all of the steady-state fluxes are scaled by the same factor:

$$J'^{\omega}_{i,j} = \alpha J^{\omega}_{i,j}, \ \forall\, i \text{ and } j. \tag{10}$$

The factor α cancels out for all of the ratios of the perturbed steady-state fluxes, and we demonstrated that

$$\frac{\partial\left(J'^{\omega}_{i,j}/J'^{\omega}_{l,n}\right)}{\partial\Delta\epsilon_m} = 0, \ \forall\, i\ (l) \text{ and } j\ (n). \tag{11}$$

Therefore, we conclude that *the ratios of stationary fluxes or any of their linear combinations do not depend on the energies of the individual states ϵ_i and only depend of barrier heights $\epsilon^{\dagger\omega}_{i,j}$.*

Illustrative Examples

To illustrate the implications of (11), we use three major biological processes: protein folding networks inspired by hen egg-white lysozyme, a KPR network for aa-tRNA selection during protein translation in the *E. Coli* ribosome, and the myosin-V motor protein that walks on the actin cytoskeleton filaments. The kinetic parameters (rate constants) that correspond to the various reactions on the corresponding biochemical networks are given in the SI Tabs. S1-S3[23,26,29–32]. For simplicity of the notation, we drop all of the prime $'$ and ω superscripts on the perturbed steady-state fluxes. We also drop the ω superscript on all of the rate constants $k_{i,j}$ except for those that correspond to multiple reactions $i \to j$ between the same two states i and j.

RESULTS

Protein Folding Network

Protein folding is a fundamental process that is required for all living cells to maintain their proper functionality. Indeed, misfolded proteins and their aggregation have been linked to many types of pathological

diseases[33]. Protein folding occurs via a series of different funnels on a free energy landscape, and as such, the process can be described using the chemical kinetic formalism for biochemical networks[14,25,26]. Protein folding often does not require any energy consumption, and therefore, it can be studied within the equilibrium thermodynamics framework[14,33]. On the other hand, in live cells all proteins are synthesized in the unfolded states and degraded/diluted in the relatively stable folded states. In this situation, a non-equilibrium steady-state distribution of fluxes in a protein folding network can give information about the relative importance of different folding pathways and the probability reaching incorrect metastable folding states.

Here, we consider a kinetic scheme representing the protein folding inspired by hen egg-white lysozyme[26,31]. For this enzyme, two mechanistic descriptions, namely, independent unrelated pathways (IUP) and pre-determined pathways with optional error (PPOE), have been proposed. The IUP model (also known as a heterogeneous folding) assumes that protein folding occurs through various intermediate states on different pathways that have no relationship to one another[25]. On the other hand, the PPOE model supposes that all proteins fold cooperatively through the same productive pathway via partially folded subunits called foldons that resemble the correctly folded structure. However, during the folding process, the protein may also become diverted into multiple misfolded error states that hinder productive folding[25].

We chose a kinetic scheme (see Fig. 2A) that combines the physicochemical aspects of both the IUP and PPOE models. There are two possible pathways for the unfolded protein in state 1 to reach the folded (native) conformation in state 3 on this biochemical kinetic network. This means that productive protein folding can proceed independently through either of the intermediate states 2 or 4. However, the protein may also become trapped in the misfolded error states denoted respectively as 5 and 6 on the two folding pathways. The misfolded error states 5 and 6 can be viewed as traps on the free-energy landscape that might kinetically block productive protein folding into the folded conformation (state 3) on the two different pathways. To realize the non-equilibrium steady state and the non-zero fluxes in this network, we assume that the protein is synthesized in state 1 and degraded from state 3 with the rate constant $k_{\varnothing,1}$. In steady state, the synthesis and degradation fluxes are balanced so that we can map this scheme to the formalism considered in the Methods by effectively introducing an irreversible $3 \to 1$ transition with the rate $k_{\varnothing,1}$.

We can now apply our analysis to ask how the steady-state folding flux splits between the pathway via state 2 ($J_1 = k_{1,2}P_1 - k_{2,1}P_2$) and via state 4 ($J_2 = k_{1,4}P_1 - k_{4,1}P_4$). (11) implies that the steady-state flux ratio will be independent of the stability of the intermediate states and is only affected by the free energy barriers. For example, consider a change in the energy of the state 2

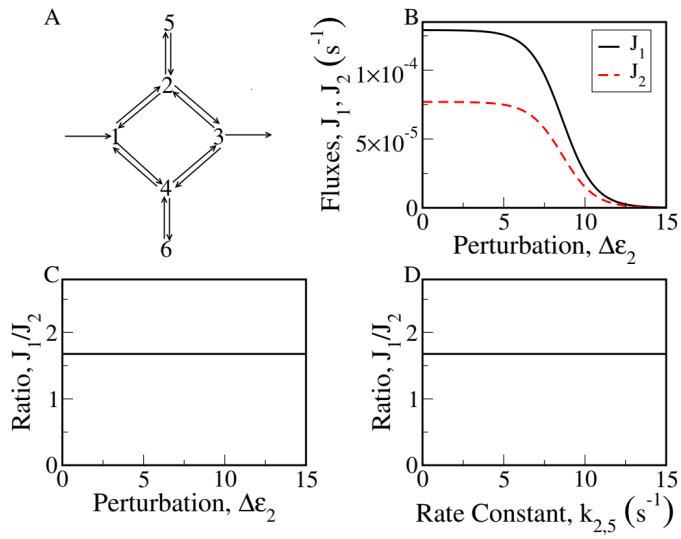

FIG. 2. Steady-state fluxes and their corresponding ratio for the biochemical network of protein folding in hen egg-white lysozyme. (A) Biochemical kinetic network for protein folding through two independent pathways to reach the folded (native) conformation in state 3 from the unfolded state 1 via the intermediates states 2 and 4, respectively. The network is based on kinetic schemes from Refs. 26,31 for protein folding under high salt conditions. (B) Steady-state fluxes J_1 and J_2 shown as a function of the energy perturbation $\Delta\epsilon_2$. Note that as the perturbation increases, both of the steady-state fluxes J_1 and J_2 decay to zero. (C) Ratio of the steady-state fluxes J_1/J_2 as a function of the energy perturbation $\Delta\epsilon_2$ on the free energy landscape. (D) Ratio of the steady-state fluxes J_1/J_2 as a function of the rate constant $k_{2,5}$ for the reaction $2 \to 5$ from the intermediate state 2 to the misfolded error state 5.

by $\Delta\epsilon_2$. This perturbation will change both J_1 and J_2 proportionally in Fig. 2B. As a result, the ratio of the steady-state fluxes J_1/J_2 does not change as a function of $\Delta\epsilon_2$ (see Fig. 2C). The result is also apparent from the analytic expression for J_1/J_2 [see the SI Eq. (S27)]. Notably, the presence of the misfolded error states 5 and 6 is mathematically equivalent to the perturbations of the energy of the states 2 and 4, respectively. Therefore, the ratio of the steady-state fluxes J_1/J_2 does not depend on the rate constant going into or out of these states (e.g., $k_{2,5}$ in Fig. 2D). Thus, the stability or presence of a misfolded error state does not affect how steady-state flux splits between the two folding pathways.

KPR Network

Enzymatic catalysis in the presence of right (cognate) and wrong (non-cognate) substrates can often achieve high selectivity through KPR mechanisms with the use of GTP/ATP hydrolysis energy. For such networks, the flux distribution can be used to quantify the probability of reaching the wrong product state (error rate) or

the probability of futile cycles that result in hydrolysis without any product formation. Here we consider a KPR network that enhances the accuracy of aa-tRNA selection in the *E. Coli* ribosome[18,27,28,32] during protein translation, and it is shown in Fig. 3*A*. It contains two symmetric cycles involving the right R (cognate) or the wrong W (noncognate) aa-tRNA molecules and two ways to reset from states 3/5 to the initials state 1. This can occur via a catalytic step resulting in product formation (rates $k^{(2)}_{3,1}/k^{(2)}_{5,1}$) or via a proofreading step that results in aa-tRNA excision (rates $k^{(1)}_{3,1}/k^{(1)}_{5,1}$). The steady-state ratios of the corresponding fluxes define important system properties of the enzyme.

The error rate can be defined as the fraction of times the non-cognate amino acid is incorporated into a protein, i.e., as a ratio of $J_W = k^{(2)}_{5,1}P_5 - k^{(2)}_{1,5}P_1$ to $J_R = k^{(2)}_{3,1}P_3 - k^{(2)}_{1,3}P_1$. Perturbations of the energy of an intermediate state (e.g., state 3 in Fig. 3*B*−*D*) will change the individual fluxes in Fig. 3*B*, but the ratio of the fluxes in Fig. 3*C* will remain invariant. This is a straightforward consequence of (11) and it generalizes the result of Ref.[24]. We can also conclude that the error rate will be invariant to perturbations of the discrete-state energies even in the presence of multiple competing pathways, multiple intermediate states, and/or multiple proofreading reactions. Therefore, the error rate in more complex KPR networks is under kinetic control as long as it can be expressed as a ratio of the steady-state fluxes in the linear chemical kinetic framework.

Energy efficiency of the ribosome can be quantified by looking at the number of GTP molecules hydrolyzed per peptide bond[18] or as the energy dissipation per product formed normalized by the GTP hydrolysis energy, i.e.,

$$\sigma_N \equiv \frac{\sigma}{J_p \Delta\mu_{\rm proof}} = \frac{J_{\rm proof}}{J_p} + \frac{\Delta\mu_p}{\Delta\mu_{\rm proof}}. \qquad (12)$$

Here, σ is the total energy dissipation in the non-equilibrium system, while $\Delta\mu_{\rm proof}$ and $\Delta\mu_p$ are the respective chemical potential differences of the proofreading and the catalytic cycles in the biochemical network. The product formation flux is $J_p = J_R + J_W$, and the proofreading flux is given by $J_{\rm proof} = k^{(1)}_{3,1}P_3 - k^{(1)}_{1,3}P_1 + k^{(1)}_{5,1}P_5 - k^{(1)}_{1,5}P_1$. The ratio of these fluxes and the normalized energy dissipation σ_N will again be invariant to the energy perturbation of an intermediate state, e.g., $\Delta\epsilon_3$ (see Fig. 3*D*).

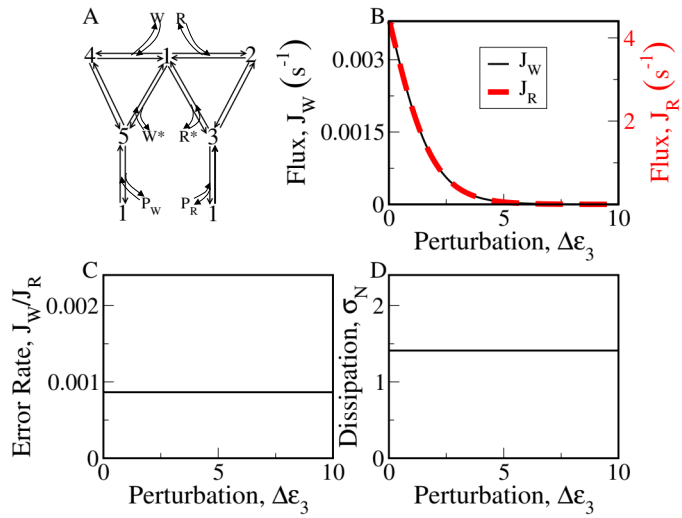

FIG. 3. Steady-state fluxes and their ratios for the biochemical network of KPR during aa-tRNA selection in the *E. Coli* ribosome. (*A*) Biochemical network for KPR in the *E. Coli* ribosome, where either the right R (cognate) or the wrong W (non-cognate) aa-tRNA molecule can bind to the free enzyme state 1. The network from kinetic schemes in Refs. 24,29,30 is comprised of two cycles: a proofreading cycle and a product formation (catalytic) cycle. Note that R* and W* respectively denote the right and wrong aa-tRNA molecules removed during proofreading with GDP also bound after GTP hydrolysis has taken place. The products P_R and P_W respectively denote the polypeptide chain elongated by either the right R or the wrong W amino acid during product formation. (*B*) Steady-state fluxes for addition of the wrong amino acid to the growing chain J_W and of the right amino acid J_R as a function of the energy perturbation $\Delta\epsilon_3$. Note that as the perturbation increases, both of the steady-state fluxes decay to zero. The red scale bar for the y-axis on the right corresponds to the red, dashed curve showing the dependence of the steady-state flux J_R on $\Delta\epsilon_3$. (*C*) Error rate for the *E. Coli* ribosome J_W/J_R as a function of $\Delta\epsilon_3$. (*D*) Normalized energy dissipation σ_N as a function of $\Delta\epsilon_3$.

Myosin-V Network

Motor proteins belong to a broad class of enzymes that convert chemical energy (e.g., from ATP hydrolysis) to perform mechanical work in cells. For example, motor proteins in cells that hydrolyze ATP use the hydrolysis energy to walk on the cytoskeletal track while transporting loads of intracellular cargo[19,20]. The motors are often described by kinetic models[20] that allow one to predict the flux distribution that defines important properties such as the probability of forward or backward steps or probability that the motor proteins hydrolyze ATP but remain at the same position on the track.

Here, for illustration we examine a kinetic model for myosin-V in Fig. 4*A* that shows the intermediate states through which the motor protein proceeds as it attempts to move one ~ 36 nm step along an actin filament[23]. The myosin-V network has a main stepping cycle (via states 1-5) where the motor protein takes one step forward or backward on the the actin filament and a futile cycle where the motor protein makes no net movement on the actin filament (via states 2, 3, 4 and 6). During the futile cycle, myosin-V does not move one step along the actin filament and all of the energy from ATP hydrolysis is wasted. This is not the case for the main stepping cycle, where myosin-V uses the energy available from ATP hy-

drolysis to take one step forward along the actin filament while doing mechanical work against a load.

The fraction of times that myosin-V takes a backward step is given by the ratio of the backward stepping flux $J_B = k_{2,1}P_2$ to the forward stepping flux $J_F = k_{1,2}P_1$. If the energy of an intermediate state is perturbed, e.g., by $\Delta\epsilon_2$, the individual fluxes J_B and J_F in Fig. 4*B* will change as well. However, the ratio of the backward to forward fluxes in Fig. 4*C* is invariant to the energy perturbation. This result is easily seen to be a consequence of (11) for the motion of the myosin-V motor protein. Moreover, we can conclude that this ratio of the backward and forward stepping fluxes will remain invariant regardless of how many intermediate states or futile cycles are present on the mechanochemical network.

The energy efficiency of myosin-V can be defined as the fraction of ATP hydrolysis energy consumed during one step on the track[20] or as the energy dissipation per step normalized by the energy expended from ATP hydrolysis, i.e.,

$$\sigma_N \equiv \frac{\sigma}{J_{\text{main}}\Delta\mu_{\text{futile}}} = \frac{J_{\text{futile}}}{J_{\text{main}}} + \frac{\Delta\mu_{\text{main}}}{\Delta\mu_{\text{futile}}}. \qquad (13)$$

Here, σ is the total energy consumed during the mechanochemical process and $\Delta\mu_{\text{futile}}$ and $\Delta\mu_{\text{main}}$ are the respective chemical potential differences of the futile cycle and the main stepping cycle. The main stepping flux is $J_{\text{main}} = k_{1,2}P_1 - k_{2,1}P_2$, and the futile flux is $J_{\text{futile}} = k_{6,2}P_6 - k_{2,6}P_2$. The ratio of these two fluxes and the normalized energy dissipation σ_N are also invariant to energy perturbations of an intermediate state such as $\Delta\epsilon_2$ on the mechanochemical cycle (see Fig. 4*D*).

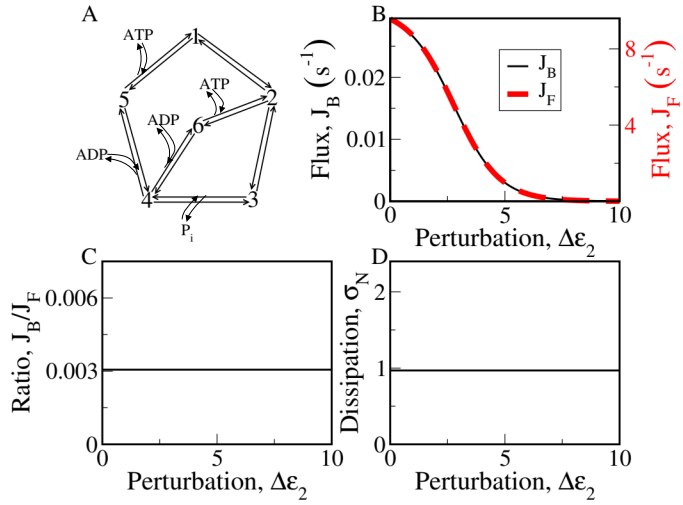

FIG. 4. Steady-state fluxes and their ratios for the mechanochemical network of the two-headed myosin-V motor protein while taking one step on an actin cytoskeleton filament. Myosin-V simultaneously hydrolyzes ATP and transports an opposing load ($F_{\text{external}} = 0.1$ pN) during this process. (*A*) Mechanochemical network for the myosin-V motor protein based on the scheme from Ref. 23 that is comprised of two cycles: a futile cycle where the motor protein remains at the same position on the actin filament and a main stepping cycle where the motor protein moves one step forward or backward along the actin filament. (*B*) Steady-state fluxes for backward steps J_B and forward steps J_F of myosin-V as a function of the energy perturbation $\Delta\epsilon_2$. Note that as the perturbation increases, both of the steady-state fluxes decay to zero. The red scale bar for the y-axis on the right corresponds to the red, dashed curve showing the dependence of the steady-state flux J_F on $\Delta\epsilon_2$. (*C*) Ratio of the backward to forward stepping fluxes J_B/J_F as a function of $\Delta\epsilon_2$. (*D*) Normalized energy dissipation σ_N as a function of $\Delta\epsilon_2$.

DISCUSSION

Our main theoretical result shows the independence of the ratios of steady-state fluxes from energy perturbations of the intermediate states of biochemical networks that describe a wide class of biological processes. This result can be explained using the following arguments. The energy perturbation at the specific site leads to a change in the stationary probability of the perturbed state and the transition rates out of the perturbed state. However, the effect of the perturbation is opposite for these two properties. If the perturbation increases (decreases) the stationary probability by the exponent of the energy perturbation, it simultaneously decreases (increases) the outgoing transition rates by the same factor. In addition, because the total probability in the system is conserved, the stationary probabilities of all of the states should be modified by the same normalization parameter. This leads to changes in all of the steady-state fluxes in the system by the same parameter, including the fluxes out of the perturbed state where the changes in the stationary probability is compensated by changes in the outgoing transition rates. As a result, all of the steady-state fluxes are scaled in the same way and their ratios remain constant.

The important implication of our theoretical results is that the properties of major biological processes that depend on the ratios of steady-state fluxes are governed by kinetic rather than thermodynamic (energetic) factors of the underlying free energy landscapes. Specifically, the ratios of any two steady-state fluxes depend on the transition state energies, but *not* on the energies of the discrete (internal) states on the free-energy landscape. Consequently, the physicochemical properties of biological systems that depend on the ratios of the steady-state fluxes are exclusively under kinetic control, and any changes in the well-depths of the individual states do not affect these properties. Therefore, the only way to modify these properties is to change the energy barriers between the intermediate states. Moreover, the invariance result is still valid if several energy perturbations are simultaneously occurring in the system because these perturbations are local and the total effect of the perturbations is additive. Note, however, that our results do not apply if the energy perturbation is also accompanied by the changes in the

free energy barriers.

To explain clearly the biological relevance of our theoretical findings, we applied them to three major biological systems, namely, protein folding via multiple pathways, aa-tRNA selection during protein translation in the *E. Coli* ribosome, and the myosin-V motor protein that walks on actin cytoskeleton filaments. Our theoretical calculations reveal some counterintuitive implications for specific experimentally observable quantities.

For the protein folding network motivated by the hen egg-white lysozyme system, we find that the splitting fractions for the different pathways along which the protein can fold do not depend on the energy (well-depths) of the intermediate states as long as the transition-state energies are constant. Mathematically, such perturbations are equivalent to the introduction of misfolded error states[25,26]. Our invariance results imply that the existence of such states or generally the existence of multistate dead-end branches from the intermediate states will not affect the splitting fractions. The results are clearly generalizable to kinetic models of protein folding in which multiple stable folding conformations are present, e.g., when there is a possibility of prion states[34]. Our results also imply that the flux splitting between the native and prion conformations would require changes in the free energy barriers and not in the well-depths along each of the folding pathways. Thus, a drug that binds to and stabilizes the intermediate but needs to dissociate before the transition states are reached cannot affect the flux splitting. We also note that energy perturbations considered here correspond to $\Phi = 0$ values in the widely utilized Φ-value analysis of protein folding transitions[35].

Our examination of the biochemical network for aa-tRNA selection in the *E. Coli* ribosome[18,21,24,29,30] demostrates that our invariance statement holds in the presence of energy-dissipating cycles on the network. We show that both the error fraction and the normalized energy dissipation can be expressed as flux ratios, and therefore, they are invariant to changes in the energies of the intermediate states on the underlying free-energy landscape. Hence, genetic mutations in the ribosome[27,32] that affect these properties must affect the kinetic features of the free energy landscape.

Finally, for the physicochemical properties of myosin-V we show that the ratio of the forward and backward stepping fluxes and the normalized energy dissipation are invariant to energy perturbations of all of the intermediate states. This indicates that the energy expenditure from ATP hydrolysis during the processive motion of the myosin-V motor protein[19,20,23] is exclusively under kinetic control as long as the external force F_{external} remains constant. Consequently, drugs that specifically stabilize different states on the mechanochemical network for myosin-V but have to dissociate before the transition to the next or to the previous state can occur do not affect the ratio of the energy efficiency or the ratio of the forward to backward steps.

Our theoretical study presents a general statement on how kinetic models that provide a quantitative description of a wide class of biological systems can be affected by the underlying features of the free-energy landscape. This result places important constraints on the mechanism for the regulation of important system-level properties. It will be important to see the implication of the invariance results for other biological systems and to determine if the result can be extended to an asymptotic flux behavior away from the steady state.

ACKNOWLEDGEMENTS

This work was supported by Center for Theoretical Biological Physics National Science Foundation (NSF) Grant PHY-1427654. A.B.K. also acknowledges support from the Welch Foundation Grant C-1559 and from NSF Grant CHE-1664218. O.A.I. also acknowledges support from the Welch Foundation Grant C-1995. We thank Qiwei Yu for useful suggestions.

AUTHOR CONTRIBUTIONS

A.B.K. and O.A.I. designed research; J.D.M., A.B.K., and O.A.I. performed research; J.D.M., A.B.K., and O.A.I. wrote the paper. *O.A.I. and A.B.K. contributed equally to this work. To whom correspondence should be addressed. E-mail: tolya@rice.edu or igoshin@rice.edu.

COMPETING INTERESTS

The authors declare no conflict of interest.

[1] I. H. Segel, *Enzyme kinetics: behavior and analysis of rapid equilibrium and steady state enzyme systems* (Wiley New York:, 1975).

[2] A. Cornish-Bowden, *Fundamentals of Enzyme Kinetics* (John Wiley & Sons, 2013).

[3] T. Kuhlman, Z. Zhang, M. H. Saier, and T. Hwa, "Combinatorial transcriptional control of the lactose operon of escherichia coli," Proc. Natl. Acad. Sci. USA **104**, 6043–6048 (2007).

[4] H. D. Kim and E. K. O'shea, "A quantitative model of transcription factor–activated gene expression," Nat. Struct. Mol. Biol. **15**, 1192 (2008).

[5] J. Narula and O. Igoshin, "Thermodynamic models of combinatorial gene regulation by distant enhancers," IET Syst. Biol. **4**, 393–408 (2010).

[6] J. Estrada, F. Wong, A. DePace, and J. Gunawardena, "Information integration and energy expenditure in gene regulation," Cell **166**, 234–244 (2016).

[7] K. L. Pierce, R. T. Premont, and R. J. Lefkowitz, "Seven-transmembrane receptors," Nat. Rev. Mol. Cell Biol. **3**, 639 (2002).

[8] J.-P. Changeux and S. J. Edelstein, "Allosteric mechanisms of signal transduction," Science **308**, 1424–1428 (2005).

[9] D. Colquhoun, "Agonist-activated ion channels," Br. J. Pharmacol. **147**, S17–S26 (2006).

[10] S. Prabakaran, G. Lippens, H. Steen, and J. Gunawardena, "Post-translational modification: nature's escape from genetic imprisonment and the basis for dynamic information encoding," Wiley Interdiscip. Rev. Syst. Biol. Med. **4**, 565–583 (2012).

[11] J. Gunawardena, "Time-scale separation–michaelis and menten's old idea, still bearing fruit," FEBS J. **281**, 473–488 (2014).

[12] J. Gunawardena, "A linear framework for time-scale separation in nonlinear biochemical systems," PloS One **7**, e36321 (2012).

[13] D. E. Makarov, *Single Molecule Science: Physical Principles and Models* (CRC Press, 2015).

[14] T. L. Hill, *Free Energy Transduction and Biochemical Cycle Kinetics* (Courier Corporation, 2005).

[15] P. Sartori and S. Pigolotti, "Kinetic versus energetic discrimination in biological copying," Phys. Rev. Lett. **110**, 188101 (2013).

[16] G. K. Ackers, A. D. Johnson, and M. A. Shea, "Quantitative model for gene regulation by lambda phage repressor," Proc. Natl. Acad. Sci. USA **79**, 1129–1133 (1982).

[17] L. Bintu, N. E. Buchler, H. G. Garcia, U. Gerland, T. Hwa, J. Kondev, and R. Phillips, "Transcriptional regulation by the numbers: models," Curr. Opin. Genet. Dev. **15**, 116–124 (2005).

[18] J. J. Hopfield, "Kinetic proofreading: A new mechanism for reducing errors in biosynthetic processes requiring high specificity," Proc. Natl. Acad. Sci. **71**, 4135–4139 (1974).

[19] J. Howard, "Molecular motors: structural adaptations to cellular functions," Nature **389**, 561–567 (1997).

[20] A. B. Kolomeisky, *Motor Proteins and Molecular Motors* (CRC Press, Taylor and Francis Group: Boca Raton, FL, 2015).

[21] J. Ninio, "Kinetic amplification of enzyme discrimination," Biochimie **57**, 587–595 (1975).

[22] A. Murugan, D. A. Huse, and S. Leibler, "Discriminatory proofreading regimes in nonequilibrium systems," Phys. Rev. X **4**, 021016 (2014).

[23] K. I. Skau, R. B. Hoyle, and M. S. Turner, "A kinetic model describing the processivity of myosin-V," Biophys. J. **91**, 2475–2489 (2006).

[24] K. Banerjee, A. B. Kolomeisky, and O. A. Igoshin, "Accuracy of substrate selection by enzymes is controlled by kinetic discrimination," J. Phys. Chem. Lett. **8**, 1552–1556 (2017).

[25] S. W. Englander, L. Mayne, and M. M. Krishna, "Protein folding and misfolding: mechanism and principles," Q. Rev. Biophys. **40**, 1–41 (2007).

[26] M. M. Krishna and S. W. Englander, "A unified mechanism for protein folding: predetermined pathways with optional errors," Protein Sci. **16**, 449–464 (2007).

[27] H. S. Zaher and R. Green, "Fidelity at the molecular level: lessons from protein synthesis," Cell **136**, 746–762 (2009).

[28] N. M. Reynolds, B. A. Lazazzera, and M. Ibba, "Cellular mechanisms that control mistranslation," Nat. Rev. Microbiol. **8**, 849 (2010).

[29] K. Banerjee, A. B. Kolomeisky, and O. A. Igoshin, "Elucidating interplay of speed and accuracy in biological error correction," Proc. Natl. Acad. Sci. USA **114**, 5183–5188 (2017).

[30] J. D. Mallory, A. B. Kolomeisky, and O. A. Igoshin, "Trade-offs between error, speed, noise, and energy dissipation in biological processes with proofreading," J. Phys. Chem. B **123**, 4718–4725 (2019).

[31] O. Bieri, G. Wildegger, A. Bachmann, C. Wagner, and T. Kiefhaber, "A salt-induced kinetic intermediate is on a new parallel pathway of lysozyme folding," Biochemistry **38**, 12460–12470 (1999).

[32] H. S. Zaher and R. Green, "Hyperaccurate and error-prone ribosomes exploit distinct mechanisms during tRNA selection," Mol. Cell **39**, 110–120 (2010).

[33] C. M. Dobson, "Protein folding and misfolding," Nature **426**, 884 (2003).

[34] S. B. Prusiner, "Prions," Proceedings of the National Academy of Sciences **95**, 13363–13383 (1998).

[35] A. R. Fersht and S. Sato, "ϕ-value analysis and the nature of protein-folding transition states," Proceedings of the National Academy of Sciences USA **101**, 7976–7981 (2004).

Supporting Information: Kinetic control of stationary flux ratios for a wide range of biochemical processes

Joel D. Mallory[†], Anatoly B. Kolomeisky[*,†,‡,§,‖], and Oleg A. Igoshin[*,†,‡,⊥]

[†] *Center for Theoretical Biological Physics, Rice University, Houston TX 77005*

[‡] *Department of Chemistry, Rice University, Houston, TX 77005*

[§] *Department of Chemical and Biomolecular Engineering, Rice University, Houston, TX 77005*

[‖] *Department of Physics and Astronomy, Rice University, Houston, TX 77005*

[⊥] *Department of Bioengineering and of Biosciences, Rice University, Houston, TX 77005*

November 27, 2019

Invariance Proof for an Arbitrary Biochemical Kinetic Network

Notation and Setup

Consider an arbitrary biochemical kinetic network with quasi-first order transitions between N biochemical states (see Fig. S1A) that is described by the linear chemical kinetic formalism[1]. The rate constant for the reaction $i \to j$ (i.e., a transition from the i-th to j-th state with $i \neq j$) is denoted by $k_{i,j}$. Note that in general there are multiple elementary reactions between the two states i and j such that the rate constant $k_{i,j}$ can be decomposed leading to

$$k_{i,j} = \sum_{\omega} k_{i,j}^{\omega}, \tag{S1}$$

where the index ω runs over all of the possible reactions $i \to j$. The occupancy probability vector $\mathbf{P}(t)$ has N components, which are the time-dependent probabilities of finding the system in a given state at time t,

$$\mathbf{P}(t) = [P_1(t), P_2(t)..., P_N(t)]^T. \tag{S2}$$

The system of forward master equations that governs the temporal evolution of the system is solved to obtain the normalized probability distribution $\mathbf{P}(t)$,

$$\frac{d\mathbf{P}(t)}{dt} = \mathbf{K} \cdot \mathbf{P}(t) \text{ and } \mathbf{1}^T \cdot \mathbf{P}(t) = 1, \tag{S3}$$

where $\mathbf{1} = [1, ..., 1]^T$ is a unit $N \times 1$ vector, and the elements of the j-th row and the i-th column of the $N \times N$ rate matrix $\mathbf{K}$ are given by

$$K_{j,i} = \begin{cases} k_{i,j}, & \text{for } j \neq i \\ -\sum_{i \neq j} k_{i,j}, & \text{for } j = i. \end{cases} \tag{S4}$$

*tolya@rice.edu, *igoshin@rice.edu

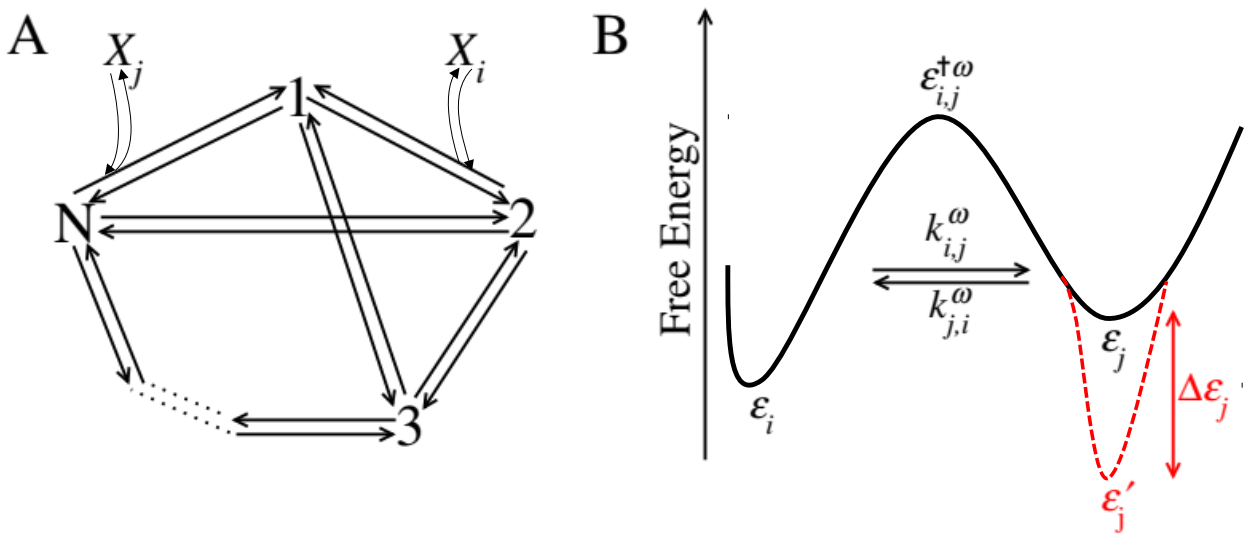

Figure S1: Representation of a general biochemical kinetic network and a portion of its free energy landscape. (A) General biochemical network comprised of N different states. The various internal states of the system are denoted by the numbers $1, .., N$, while the cofactor molecules in the bath that are involved in the various bimolecular reactions have chemical identities denoted by X_i and X_j, respectively. (B) A portion of a free energy landscape corresponding to the reaction between the states i and j with the energies of the respective intermediate states (well-depths) denoted by ϵ_i and ϵ_j and the transition state energy denoted by $\epsilon_{i,j}^{\dagger\omega}$. The respective rate constants $k_{i,j}^{\omega}$ and $k_{j,i}^{\omega}$ correspond to the forward and reverse reactions between the two states i and j on the pathway ω. Note that the energy of the state j is decreased (perturbed) by an amount $\Delta\epsilon_j$ (red, dashed curve) such that the energy of the perturbed state is $\epsilon_j' = \epsilon_j - \Delta\epsilon_j$.

In the limit of the time $t \to \infty$, the system approaches a non-equilibrium steady-state denoted by the stationary occupancy probability vector $\mathbf{P}$ such that

$$\mathbf{K} \cdot \mathbf{P} = \mathbf{0} \text{ and } \mathbf{1}^T \cdot \mathbf{P} = 1. \tag{S5}$$

Assuming that the matrix $\mathbf{K}$ is not rank deficient, these equations define a unique solution to the set of steady-state forward master equations, i.e., the stationary probability distribution $\mathbf{P}$. Note that the stationary probability distribution $\mathbf{P}$ would be the Boltzmann distribution if the system approached thermodynamic equilibrium in the limit of $t \to \infty$. In this case, the probability of the individual states is known immediately as $P_i = e^{-\epsilon_i}/Z$, where ϵ_i is the energy of the state and $Z = \sum_i e^{-\epsilon_i}$ is the partition function from statistical mechanics[2].

Kramer's Law

Consider the arbitrary biochemical kinetic network in Fig. S1A with N internal states that define the system contained within a bath (i.e., the cellular environment) of chemical species defined as cofactor molecules with chemical identities X_γ. The steady-state of the system defined in Eq. (S5) will change in response to chemical reactions occurring between the internal states that affect the energies ϵ_γ (in units of $k_B T$) of the cofactor molecules in the bath. The rate constants $k_{i,j}^{\omega}$ corresponding to the reactions $i \to j$ in the system follow Kramer's law such that they can be decomposed and expressed in Kramer's form as

$$k_{i,j}^{\omega} = k_i^0 e^{\epsilon_i - \epsilon_{i,j}^{\dagger\omega}}. \tag{S6}$$

Here, k_i^0 is a pre-exponential (frequency) factor independent of the energies of the internal states in the system, while ϵ_i and $\epsilon_{i,j}^{\dagger\omega} = \epsilon_{j,i}^{\dagger\omega}$ are the respective energies of the internal and the transition states on the free energy landscape of the system.

However, the energies ϵ_γ of the cofactor molecules in the bath must be projected onto the internal states of the system (i.e., the biochemical kinetic network). Thus, any rate constants $k^\omega_{i,j}$ for bimolecular and higher order reactions in the system that cause changes in the energy ϵ_γ of the cofactor molecule X_γ due to a binding reaction are modified by a prefactor $e^{\sum_\gamma \nu_\gamma \mu_\gamma}$. The prefactor effectively raises the energy ϵ_i of the internal state and reduces the barrier for the reaction by $\sum_\gamma \nu_\gamma \mu_\gamma$. Specifically, ν_γ is the stochiometric coefficient denoting the number of cofactor molecules X_γ that are consumed during the binding reaction such that $\nu_\gamma = 0$ if no cofactor molecule X_γ participates in the reaction. Moreover, $\mu_\gamma \equiv \Delta\epsilon_\gamma$ is the fixed chemical potential defined as the energy change per cofactor molecule X_γ during a binding reaction that consumes this species[3]. Note also that if the biological process involves a mechanochemical cycle for a motor protein, the rate constant is modified by a prefactor of $e^{F_{\text{external}} d_{\text{step}}}$ for the elementary reaction where the mechanical work is performed. In this case, F_{external} is the opposing force due to the external load from the intracellular cargo and d_{step} is the distance that the motor protein moves in one step on the cytoskeleton track[4].

The modification of the unimolecular prefactors k^0_i for the binding reactions of the cofactor molecules X_γ enables the rate constants to be written as

$$k^\omega_{i,j} = k^0_i e^{\sum_\gamma \nu_\gamma \mu_\gamma} e^{\epsilon_i - \epsilon^{\dagger\omega}_{i,j}}. \tag{S7}$$

The prefactor $e^{\sum_\gamma \nu_\gamma \mu_\gamma}$ is treated as a constant because it corresponds to changes in the energies of the cofactor molecules in the bath and not to changes in the energies of the internal states of the system. Therefore, a new set of pre-exponential factors $k^{0\omega}_{i,j}$ can be defined with the prefactor absorbed into them,

$$k^{0\omega}_{i,j} \equiv k^0_i e^{\sum_\gamma \nu_\gamma \mu_\gamma}. \tag{S8}$$

This leads to the following generalized Kramer's expression for all of the rate constants $k^\omega_{i,j}$ of the elementary reactions on the biochemical network,

$$k^\omega_{i,j} = k^{0\omega}_{i,j} e^{\epsilon_i - \epsilon^{\dagger\omega}_{i,j}}. \tag{S9}$$

Generalized Detailed Balance Constraints

Consider an arbitrary cycle on a biochemical network with a chemical potential difference (i.e., a thermodynamic force) $\Delta\mu_{\text{cycle}}$. The generalized detailed balance constraint in terms of the rate constants for the clockwise $k^\omega_{i,j}$ and counterclockwise $k^\omega_{j,i}$ directions of the cycle is given by

$$\Delta\mu_{\text{cycle}} = \ln\left(\prod_i \frac{k^\omega_{i,j}}{k^\omega_{j,i}}\right). \tag{S10}$$

Using Eq. (S7) for the rate constants $k^\omega_{i,j}$ in this equation, it is easy to see that $\Delta\mu_{\text{cycle}}$ defines the chemical potential difference between all of the cofactor X_α (substrate) and X_β (product) molecules that participate in the binding and dissociation reactions of the cycle,

$$\Delta\mu_{\text{cycle}} \equiv \sum_\alpha \nu_\alpha \mu_\alpha - \sum_\beta \nu_\beta \mu_\beta. \tag{S11}$$

Note also that using the generalized Kramer's expression for the rate constants from Eq. (S9) in Eq. (S10) leads to the following equation for the chemical potential difference,

$$\Delta\mu_{\text{cycle}} = \ln\left(\prod_i \frac{k^{0\omega}_{i,j}}{k^{0\omega}_{j,i}}\right). \tag{S12}$$

Substitution of the prefactors $k^{0\omega}_{i,j}$ defined in Eq. (S8) into this equation gives the defintion for the chemical potential difference over the cycle in Eq. (S11). Therefore, the generalized detailed balance constraint for the cycles of biochemical networks arises naturally as a consequence of the linear chemical kinetic formalism.

If the cycle does not change the chemical composition of the bath, it obeys the detailed balance constraint such that the chemical potential difference over the cycle $\Delta\mu_{\text{cycle}} = 0$. This implies that when the cycle runs,

e.g., in the clockwise direction, binding of a cofactor molecule X_α is compensated by the dissociation of the same molecule $X_\beta = X_\alpha$ such that the species is not chemically modified upon completion of the cycle. If the cycle runs in the counterclockwise (i.e., the reverse) direction, the dissociation of the cofactor molecule $X_\beta = X_\alpha$ would be a binding reaction and visa-versa. In this scenario, the prefactors cancel out because they are the same (i.e., $e^{\sum_\alpha \nu_\alpha \mu_\alpha - \sum_\beta \nu_\beta \mu_\beta} = 1$) regardless of whether the cycle proceeds in the clockwise or counterclockwise directions. Therefore, cycles at thermodynamic equilibrium do not change the chemical composition of the cofactor molecules in the bath. However, if the cycle does change the chemical composition of the bath, the chemical potential difference over the cycle $\Delta\mu_{\text{cycle}} \neq 0$, and the cycle violates the detailed balance constraint. In this situation, binding of the cofactor molecule X_α results in the production of a new cofactor molecule X_β upon completion of the cycle. Thus, the respective prefactors for the clockwise and counterclockwise directions of the cycle are not the same, and the cycle affects the concentrations of the species $[X_\alpha]$ and $[X_\beta]$ in the bath. For dilute solutions of cofactor molecules (e.g., X_α) the chemical potential depends explicitly on the concentration $[X_\alpha]$,

$$\mu_\alpha = \mu_\alpha^\circ + \ln([X_\alpha]), \tag{S13}$$

where μ_α° is the chemical potential of the cofactor molecules X_α when the concentration of this species is 1 M. Here, it is clear that the prefactor for the binding reaction is proportional to $[X_\alpha]^{\nu_\alpha}$ [2]. Using Eq. (S13) in Eq. (S11), the chemical potential difference over the cycle is given by

$$\Delta\mu_{\text{cycle}} = \Delta\mu_{\text{cycle}}^\circ + \ln\left(\frac{\prod_\alpha [X_\alpha]^{\nu_\alpha}}{\prod_\beta [X_\beta]^{\nu_\beta}}\right). \tag{S14}$$

For example, the production of the new cofactor molecule X_β during the cycle may lead to changes in the concentrations of other energy-rich molecules such as [ATP] and its hydrolysis products [ADP] and [P_i] such that the chemical potential difference for ATP hydrolysis is given by

$$\Delta\mu_{\text{ATP}} = \Delta\mu_{\text{ATP}}^\circ + \ln\left(\frac{[\text{ATP}]}{[\text{ADP}][\text{P}_\text{i}]}\right). \tag{S15}$$

Consequently, the composition of the bath changes for a cycle in a non-equilibirum steady-state due to chemical modification of the cofactor molecule X_α to X_β and/or energy expenditure from ATP hydrolysis. This result demonstrates that the generalized Kramer's expressions for the rate constants in the linear chemical kinetic formalism provide a way to properly account for the detailed balance constraints of the cycles on biochemical networks.

Perturbation of the Free Energy Landscape

Consider a perturbation that decreases the energy of an arbitrary state m on the free energy landscape of the system by an amount $\Delta\epsilon_m$ (in units of k_BT) such that $\epsilon'_m = \epsilon_m - \Delta\epsilon_m$, while all of the energies of the other intermediate states $i \neq m$ remain unperturbed (see Fig. S1B). Moreover, all of the transition state energies $\epsilon_{i,j}^{\dagger\omega}$ and the energies ϵ_γ of all of the cofactor molecules are held constant. The perturbation of the state m reduces all of the rate constants $k_{m,j}^\omega$ for the reactions $m \to j$ by a factor of $e^{-\Delta\epsilon_m}$, but all of the other rate constants $k_{i,j}^\omega$ remain the same. Therefore, the rate constants $k_{i,j}^{'\omega}$ after energy perturbation of the state m are denoted by

$$k_{i,j}^{'\omega} = \begin{cases} k_{i,j}^\omega, & \text{for } i \neq m \\ k_{m,j}^\omega e^{-\Delta\epsilon_m}, & \text{for } i = m. \end{cases} \tag{S16}$$

This leads to the scaling of the entire m-th column of the perturbed rate matrix $\mathbf{K'}$ by the factor of $e^{-\Delta\epsilon_m}$ such that

$$K'_{j,i} = \begin{cases} K_{j,i}, & \text{for } i \neq m \\ K_{j,m} e^{-\Delta\epsilon_m}, & \text{for } i = m. \end{cases} \tag{S17}$$

We can denote the new steady-state probability distribution as $\mathbf{P'}$, and it must satisfy the following set of steady-state forward master equations and obey the conservation of probability,

$$\mathbf{K'} \cdot \mathbf{P'} = \mathbf{0} \text{ and } \mathbf{1}^T \cdot \mathbf{P'} = 1. \tag{S18}$$

The perturbed probabilities can be expressed in terms of unperturbed probabilities according to

$$P_i' = \begin{cases} \alpha P_i, & \text{for } i \neq m \\ \alpha P_m e^{\Delta\epsilon_m}, & \text{for } i = m, \end{cases} \tag{S19}$$

where α is a normalization constant,

$$\alpha = \frac{1}{\sum_{j\neq k} P_j + P_m e^{\Delta\epsilon_m}}. \tag{S20}$$

This choice of normalization constant guarantees that the conservation of probability is satisfied such that $\mathbf{1}^T \cdot \mathbf{P'} = 1$. Also, we must show that $\mathbf{K'} \cdot \mathbf{P'} = \mathbf{0}$ by considering the j-th row of the vector equality

$$\begin{aligned} \sum_{i=1}^{N} K'_{j,i} P'_i &= \sum_{i=1, i\neq m}^{N} K'_{j,i} P'_i + K'_{j,m} P'_m \\ &= \sum_{i=1, i\neq m}^{N} K_{j,i} P_i + K_{j,m} e^{-\Delta\epsilon_m} P_m e^{\Delta\epsilon_m} \\ &= \sum_{i=1}^{N} K_{j,i} P_i = 0. \end{aligned} \tag{S21}$$

Invariance of the Ratios of the Steady-State Fluxes

By denoting $J^{\omega}_{i,j}$ as the steady-state flux of the reaction $i \to j$, we determine the relationship between the unperturbed steady-state flux $J^{\omega}_{i,j}$ and the perturbed steady-state flux $J'^{\omega}_{i,j}$. All of the unperturbed steady-state fluxes $J^{\omega}_{i,j}$ are scaled by the same factor α such that the perturbed steady-state fluxes $J'^{\omega}_{i,j}$ are given by

$$J'^{\omega}_{i,j} = \alpha J^{\omega}_{i,j}, \ \forall\, i \text{ and } j. \tag{S22}$$

The unperturbed steady-state flux is $J^{\omega}_{i,j} = k^{\omega}_{i,j} P_i$, and the perturbed steady-state flux is $J'^{\omega}_{i,j} = k'^{\omega}_{i,j} P'_i$ such that using the Eq. (S16) for $k'^{\omega}_{i,j}$ we obtain

$$J'^{\omega}_{i,j} = \begin{cases} k^{\omega}_{i,j} P'_i, & \text{for } i \neq m \\ k^{\omega}_{m,j} e^{-\Delta\epsilon_m} P'_m, & \text{for } i = m, \end{cases} \tag{S23}$$

which can be expressed in terms of the unperturbed probabilities P_i (see Eq. (S19)) as

$$J'^{\omega}_{i,j} = \begin{cases} \alpha k^{\omega}_{i,j} P_i, & \text{for } i \neq m \\ \alpha k^{\omega}_{m,j} e^{-\Delta\epsilon_m} P_m e^{\Delta\epsilon_m}, & \text{for } i = m. \end{cases} \tag{S24}$$

Due to the cancellation of the exponential terms involving the energy perturbation $\Delta\epsilon_m$, we have shown that

$$J'^{\omega}_{i,j} = \alpha k^{\omega}_{i,j} P_i = \alpha J^{\omega}_{i,j}, \ \forall\, i \text{ and } j. \tag{S25}$$

Note that the factor α cancels out for all of the ratios of the steady-state fluxes,

$$\frac{J'^{\omega}_{i,j}}{J'^{\omega}_{l,n}} = \frac{J^{\omega}_{i,j}}{J^{\omega}_{l,n}}, \ \forall\, i\ (l) \text{ and } j\ (n), \tag{S26}$$

(and hence, for any linear combination of the fluxes) such that they are invariant to the energy perturbation $\Delta\epsilon_m$ of the m-th intermediate state on the free energy landscape. Therefore, we demonstrated that

$$\frac{\partial\left(J'^{\omega}_{i,j}/J'^{\omega}_{l,n}\right)}{\partial\Delta\epsilon_m} = 0, \ \forall\, i\ (l) \text{ and } j\ (n). \tag{S27}$$

Protein Folding Network

Table. S1 lists the kinetic parameters for the protein folding network motivated by folding pathways in the hen egg-white lysozyme[5,6] (see Fig. $2A-D$ in the main text). The unfolded protein in state 1 can reach the folded (native) conformation in state 3 along two possible pathways via the intermediate states 2 and 4. However, the protein may also become trapped in the misfolded error states 5 and 6, respectively. The correctly folded conformation (state 3) is degraded with a steady-state flux $J_{\varnothing,1} = k_{\varnothing,1}P_3$ such that there is an additional pathway $3 \to 1$ between the folded state 3 and the unfolded state 1. Consequently, the protein folding network is in a non-equilibrium steady-state where the folded proteins are degraded with a rate $k_{\varnothing,1}$.

Kinetic Parameters: Protein Folding in Hen Egg-White Lysozyme

Table S1: Rate Constants $k_{i,j}$ for Protein Folding motivated by Hen Egg-White Lysozyme.

System Parameters	Protein Folding
$k_{1,2}$	14
$k_{2,1}$	0.4
$k_{1,4}$	6.2
$k_{4,1}$	5×10^{-5}
$k_{2,3}$	0.7
$k_{3,2}$	6×10^{-9}
$k_{4,3}$	3×10^{-4}
$k_{3,4}$	5×10^{-7}
$k_{2,5}$	2.4×10^{-4}
$k_{5,2}$	9.2
$k_{4,6}$	2.2×10^{-4}
$k_{6,4}$	4.4
$k_{\varnothing,1}$	2.8×10^{-4}

The values of the rate constants $k_{i,j}$ (in units of s^{-1}) for protein folding (except for $k_{2,5}$, $k_{4,6}$, and $k_{\varnothing,1}$) are from experimental folding data reported in Refs. 6,7 under high salt conditions.

Analytic Expression: Ratio of the Steady-State Fluxes

The ratio of the steady-state fluxes J_1/J_2 expressed in a generalized Kramer's form (see Eq. (S9)) does not depend on the energies of any of the intermediate states ϵ_i. The analytic expression for this ratio of the fluxes depends only on the transition state energies $\epsilon^{\dagger}_{i,j}$:

$$\frac{J_1}{J_2} = \frac{k^0_{2,3}k^0_{3,\varnothing}k^0_{4,1}k^0_{1,2}e^{\epsilon^{\dagger}_{4,3}} + e^{\epsilon^{\dagger}_{3,\varnothing}}\left(k^0_{2,3}k^0_{4,3}k^0_{4,1}k^0_{1,2} - k^0_{2,3}k^0_{4,3}k^0_{2,1}k^0_{1,4}\right) + k^0_{2,3}k^0_{4,3}k^0_{3,\varnothing}k^0_{1,2}e^{\epsilon^{\dagger}_{1,4}}}{k^0_{4,3}k^0_{3,\varnothing}k^0_{2,1}k^0_{1,4}e^{\epsilon^{\dagger}_{2,3}} + e^{\epsilon^{\dagger}_{3,\varnothing}}\left(k^0_{2,3}k^0_{4,3}k^0_{2,1}k^0_{1,4} - k^0_{2,3}k^0_{4,3}k^0_{4,1}k^0_{1,2}\right) + k^0_{2,3}k^0_{4,3}k^0_{3,\varnothing}k^0_{1,4}e^{\epsilon^{\dagger}_{1,2}}}. \tag{S28}$$

This is a consequence of Eq. (11) in the main text for the ratio of the steady-state fluxes J_1/J_2 for the two possible pathways on the protein folding network.

KPR Network

Table. S2 lists the kinetic parameters for the kinetic proofreading (KPR) network that describes aminoacyl(aa)-tRNA selection in the *E. coli* ribosome (see Fig. $3A-D$ in the main text). This KPR process is an important step during protein translation[8,9], and it is performed by the ribosome with high fidelity (error rate $\sim 10^{-3} - 10^{-4}$)[10–14]. The biochemical network is comprised of two cycles powered by GTP hydrolysis that involve the right R (cognate)/wrong W (non-cognate) aa-tRNA molecules. This process has a product formation cycle (rates $k^{(2)}_{3,1}/k^{(2)}_{5,1}$) where one amino acid is added to the growing polypeptide chain to create

the products P_R/P_W and a proofreading cycle (rates $k^{(1)}_{3,1}/k^{(1)}_{5,1}$) where an aa-tRNA molecule is excised from the ribosome to give R*/W*.

Kinetic Parameters: aa-tRNA Selection in the *E. coli* Ribosome

Table S2: Experimental Rate Constants $k_{i,j}$ for aa-tRNA Selection in the *E. coli* Ribosome

System Parameters	*E. coli* Ribosome
$k_{1,2}$	40
$k_{2,1}$	0.5
$k_{2,3}$	25
$k_{3,2}$	1×10^{-3}
$k^{(1)}_{3,1}$	8.5×10^{-2}
$k^{(1)}_{1,3}$	1×10^{-3}
$k^{(2)}_{3,1}$	8.415
$k^{(2)}_{1,3}$	6.9×10^{-5}
$k_{1,4}$	27
$k_{4,1}$	47
$k_{4,5}$	1.2
$k_{5,4}$	1×10^{-3}
$k^{(1)}_{5,1}$	0.67
$k^{(1)}_{1,5}$	2.7×10^{-6}
$k^{(2)}_{5,1}$	3.5×10^{-2}
$k^{(2)}_{1,5}$	9.9×10^{-11}

The values of the rate constants $k_{i,j}$ (in units of s^{-1}) are from experimental data reported in Ref. 11. The chemical potential differences from Ref. 14 for the respective proofreading and the product formation cycles are fixed at their physiological values for GTP hydrolysis $\Delta\mu_{\text{proof}} \sim 20\ k_BT$ and product formation $\Delta\mu_{\text{p}} \sim 26\ k_BT$. Note also that $\Delta\mu_{\text{proof}}$ and $\Delta\mu_{\text{p}}$ for the proofreading and the product formation cycles are equal for the right R (cognate) and wrong W (non-cognate) aa-tRNA molecules.

Analytic Expressions: Error Rate and Normalized Energy Dissipation

The error rate is the probability that a wrong W amino acid is added to the growing polypeptide chain. This ratio of the wrong W product formation flux J_W to the right R product formation flux J_R written in a generalized Kramer's form is:

$$\frac{J_W}{J_R} = \Bigg[\left(k^0_{2,1} k^{0(2)}_{3,1} e^{\epsilon^{\dagger(1)}_{3,1} + \epsilon_{2,3}{}^{\dagger}} + k^0_{2,3} k^{0(2)}_{3,1} e^{\epsilon^{\dagger(1)}_{3,1} + \epsilon_{1,2}{}^{\dagger}} + k^0_{2,1} k^{0(1)}_{3,1} e^{\epsilon^{\dagger(2)}_{3,1} + \epsilon_{2,3}{}^{\dagger}} + k^0_{2,3} k^{0(1)}_{3,1} e^{\epsilon^{\dagger(2)}_{3,1} + \epsilon_{1,2}{}^{\dagger}} + k^0_{2,1} k^0_{3,2} e^{\epsilon^{\dagger(1)}_{3,1} + \epsilon^{\dagger(2)}_{3,1}} \right)$$
$$\left(k^0_{4,1} \left(k^{0(2)}_{1,5} k^{(1)}_{5,1} - k^{0(1)}_{1,5} k^{0(2)}_{5,1} \right) e^{\epsilon_{4,5}{}^{\dagger}} + k^0_{4,5} \left(k^{0(2)}_{1,5} k^{0(1)}_{5,1} - k^{0(1)}_{1,5} k^{0(2)}_{5,1} \right) e^{\epsilon_{1,4}{}^{\dagger}} + \left(k^{0(2)}_{1,5} k^0_{4,1} k^0_{5,4} - k^0_{1,4} k^0_{4,5} k^{0(2)}_{5,1} \right) e^{\epsilon^{\dagger(1)}_{5,1}} \right) \Bigg] \Bigg/$$
$$\Bigg[\left(k^0_{2,1} \left(k^{0(2)}_{1,3} k^{0(1)}_{3,1} - k^{0(1)}_{1,3} k^{0(2)}_{3,1} \right) e^{\epsilon_{2,3}{}^{\dagger}} + k^0_{2,3} \left(k^{0(2)}_{1,3} k^{0(1)}_{3,1} - k^{0(1)}_{1,3} k^{0(2)}_{3,1} \right) e^{\epsilon_{1,2}{}^{\dagger}} + \left(k^{0(2)}_{1,3} k^0_{2,1} k^0_{3,2} - k^0_{1,2} k^0_{2,3} k^{0(2)}_{3,1} \right) e^{\epsilon^{\dagger(1)}_{3,1}} \right)$$
$$\left(k^0_{4,1} k^{0(2)}_{5,1} e^{\epsilon^{\dagger(1)}_{5,1} + \epsilon_{4,5}{}^{\dagger}} + k^0_{4,5} k^{0(2)}_{5,1} e^{\epsilon^{\dagger(1)}_{5,1} + \epsilon_{1,4}{}^{\dagger}} + k^0_{4,1} k^{0(1)}_{5,1} e^{\epsilon^{\dagger(2)}_{5,1} + \epsilon_{4,5}{}^{\dagger}} + k^0_{4,5} k^{0(1)}_{5,1} e^{\epsilon^{\dagger(2)}_{5,1} + \epsilon_{1,4}{}^{\dagger}} + k^0_{4,1} k^0_{5,4} e^{\epsilon^{\dagger(1)}_{5,1} + \epsilon^{\dagger(2)}_{5,1}} \right) \Bigg].$$

Notably, the error rate depends only on the transition state energies $\epsilon^{\dagger}_{i,j}$, but it does not depend on the energies ϵ_i of any intermediate states. As such, the error rate is invariant to energy perturbations of the intermediate states on the free energy landscape. In addition, the normalized energy dissipation σ_N (see Eq. (12) in the main text) depends on the ratio of the proofreading to the product formation fluxes J_{proof}/J_p, and this property is also invariant to the energy perturbations of the intermediate states. The following analytic expression for the normalized energy dissipation written in a generalized Kramer's form depends

only on the transition state energies $\epsilon^{\dagger}_{i,j}$:

$$
\begin{aligned}
\sigma_N = -\Bigg[& e^{\epsilon^{\dagger(1)}_{3,1}+\epsilon_{2,3}{}^{\dagger}+\epsilon_{4,5}{}^{\dagger}} k^0_{2,1}k^0_{4,1}\left(k^{0(2)}_{1,5}k^{0(1)}_{5,1}-k^{0(1)}_{1,5}k^{0(2)}_{5,1}\right)k^{0(2)}_{3,1} + e^{\epsilon^{\dagger(1)}_{3,1}+\epsilon_{1,2}{}^{\dagger}+\epsilon_{4,5}{}^{\dagger}} k^0_{2,3}k^0_{4,1}\left(k^{0(2)}_{1,5}k^{0(1)}_{5,1}-k^{0(1)}_{1,5}k^{0(2)}_{5,1}\right)k^{0(2)}_{3,1} \\
& + e^{\epsilon^{\dagger}_{3,1}+\epsilon_{1,4}{}^{\dagger}+\epsilon_{2,3}{}^{\dagger}} k^0_{2,1}k^0_{4,5}\left(k^{0(2)}_{1,5}k^{0(1)}_{5,1}-k^{0(1)}_{1,5}k^{0(2)}_{5,1}\right)k^{0(2)}_{3,1} + e^{\epsilon^{\dagger(1)}_{3,1}+\epsilon_{1,2}{}^{\dagger}+\epsilon_{1,4}{}^{\dagger}} k^0_{2,3}k^0_{4,5}\left(k^{0(2)}_{1,5}k^{0(1)}_{5,1}-k^{0(1)}_{1,5}k^{0(2)}_{5,1}\right)k^{0(2)}_{3,1} \\
& + e^{\epsilon^{\dagger(1)}_{3,1}+\epsilon^{\dagger(2)}_{5,1}+\epsilon_{2,3}{}^{\dagger}} k^0_{2,1}\left(k^0_{1,4}k^0_{4,5}k^{0(1)}_{5,1}-k^{0(1)}_{1,5}k^0_{4,1}k^0_{5,4}\right)k^{0(2)}_{3,1} + e^{\epsilon^{\dagger(1)}_{3,1}+\epsilon^{\dagger(2)}_{5,1}+\epsilon_{1,2}{}^{\dagger}} k^0_{2,3}\left(k^0_{1,4}k^0_{4,5}k^{0(1)}_{5,1}-k^{0(1)}_{1,5}k^0_{4,1}k^0_{5,4}\right)k^{0(2)}_{3,1} \\
& + e^{\epsilon^{\dagger(2)}_{3,1}+\epsilon_{2,3}{}^{\dagger}+\epsilon_{4,5}{}^{\dagger}} k^0_{2,1}k^0_{4,1}\left(k^{0(2)}_{1,5}k^{0(1)}_{5,1}-k^{0(1)}_{1,5}k^{0(2)}_{5,1}\right)k^{0(1)}_{3,1} + e^{\epsilon^{\dagger(2)}_{3,1}+\epsilon_{1,2}{}^{\dagger}+\epsilon_{4,5}{}^{\dagger}} k^0_{2,3}k^0_{4,1}\left(k^{0(2)}_{1,5}k^{0(1)}_{5,1}-k^{0(1)}_{1,5}k^{0(2)}_{5,1}\right)k^{0(1)}_{3,1} \\
& + e^{\epsilon^{\dagger(2)}_{3,1}+\epsilon_{1,4}{}^{\dagger}+\epsilon_{2,3}{}^{\dagger}} k^0_{2,1}k^0_{4,5}\left(k^{0(2)}_{1,5}k^{0(1)}_{5,1}-k^{0(1)}_{1,5}k^{0(2)}_{5,1}\right)k^{0(1)}_{3,1} + e^{\epsilon^{\dagger(2)}_{3,1}+\epsilon_{1,2}{}^{\dagger}+\epsilon_{1,4}{}^{\dagger}} k^0_{2,3}k^0_{4,5}\left(k^{0(2)}_{1,5}k^{0(1)}_{5,1}-k^{0(1)}_{1,5}k^{0(2)}_{5,1}\right)k^{0(1)}_{3,1} \\
& + e^{\epsilon^{\dagger(2)}_{3,1}+\epsilon^{\dagger(2)}_{5,1}+\epsilon_{2,3}{}^{\dagger}} k^0_{2,1}\left(k^0_{1,4}k^0_{4,5}k^{0(1)}_{5,1}-k^{0(1)}_{1,5}k^0_{4,1}k^0_{5,4}\right)k^{0(1)}_{3,1} + e^{\epsilon^{\dagger(2)}_{3,1}+\epsilon^{\dagger(2)}_{5,1}+\epsilon_{1,2}{}^{\dagger}} k^0_{2,3}\left(k^0_{1,4}k^0_{4,5}k^{0(1)}_{5,1}-k^{0(1)}_{1,5}k^0_{4,1}k^0_{5,4}\right)k^{0(1)}_{3,1} \\
& + e^{\epsilon^{\dagger(1)}_{5,1}+\epsilon_{2,3}{}^{\dagger}+\epsilon_{4,5}{}^{\dagger}} k^0_{2,1}\left(k^{0(2)}_{1,3}k^{0(1)}_{3,1}-k^{0(1)}_{1,3}k^{0(2)}_{3,1}\right)k^0_{4,1}k^{0(2)}_{5,1} + e^{\epsilon^{\dagger(1)}_{5,1}+\epsilon_{1,2}{}^{\dagger}+\epsilon_{4,5}{}^{\dagger}} k^0_{2,3}\left(k^{0(2)}_{1,3}k^{0(1)}_{3,1}-k^{0(1)}_{1,3}k^{0(2)}_{3,1}\right)k^0_{4,1}k^{0(2)}_{5,1} \\
& + e^{\epsilon^{\dagger(1)}_{5,1}+\epsilon^{\dagger(2)}_{3,1}+\epsilon_{4,5}{}^{\dagger}}\left(k^0_{1,2}k^0_{2,3}k^{0(1)}_{3,1}-k^{0(1)}_{1,3}k^0_{2,1}k^0_{3,2}\right)k^0_{4,1}k^{0(2)}_{5,1} + e^{\epsilon^{\dagger(1)}_{5,1}+\epsilon_{1,4}{}^{\dagger}+\epsilon_{2,3}{}^{\dagger}} k^0_{2,1}\left(k^{0(2)}_{1,3}k^{0(1)}_{3,1}-k^{0(1)}_{1,3}k^{0(2)}_{3,1}\right)k^0_{4,5}k^{0(2)}_{5,1} \\
& + e^{\epsilon^{\dagger(1)}_{5,1}+\epsilon_{1,2}{}^{\dagger}+\epsilon_{1,4}{}^{\dagger}} k^0_{2,3}\left(k^{0(2)}_{1,3}k^{0(1)}_{3,1}-k^{0(1)}_{1,3}k^{0(2)}_{3,1}\right)k^0_{4,5}k^{0(2)}_{5,1} + e^{\epsilon^{\dagger(1)}_{5,1}+\epsilon^{\dagger(2)}_{3,1}+\epsilon_{1,4}{}^{\dagger}}\left(k^0_{1,2}k^0_{2,3}k^{0(1)}_{3,1}-k^{0(1)}_{1,3}k^0_{2,1}k^0_{3,2}\right)k^0_{4,5}k^{0(2)}_{5,1} \\
& + e^{\epsilon^{\dagger(2)}_{5,1}+\epsilon_{2,3}{}^{\dagger}+\epsilon_{4,5}{}^{\dagger}} k^0_{2,1}\left(k^{0(2)}_{1,3}k^{0(1)}_{3,1}-k^{0(1)}_{1,3}k^{0(2)}_{3,1}\right)k^0_{4,1}k^{0(1)}_{5,1} + e^{\epsilon^{\dagger(2)}_{5,1}+\epsilon_{1,2}{}^{\dagger}+\epsilon_{4,5}{}^{\dagger}} k^0_{2,3}\left(k^{0(2)}_{1,3}k^{0(1)}_{3,1}-k^{0(1)}_{1,3}k^{0(2)}_{3,1}\right)k^0_{4,1}k^{0(1)}_{5,1} \\
& + e^{\epsilon^{\dagger(2)}_{3,1}+\epsilon^{\dagger(2)}_{5,1}+\epsilon_{4,5}{}^{\dagger}}\left(k^0_{1,2}k^0_{2,3}k^{0(1)}_{3,1}-k^{0(1)}_{1,3}k^0_{2,1}k^0_{3,2}\right)k^0_{4,1}k^{0(1)}_{5,1} + e^{\epsilon^{\dagger(2)}_{5,1}+\epsilon_{1,4}{}^{\dagger}+\epsilon_{2,3}{}^{\dagger}} k^0_{2,1}\left(k^{0(2)}_{1,3}k^{0(1)}_{3,1}-k^{0(1)}_{1,3}k^{0(2)}_{3,1}\right)k^0_{4,5}k^{0(1)}_{5,1} \\
& + e^{\epsilon^{\dagger(2)}_{5,1}+\epsilon_{1,2}{}^{\dagger}+\epsilon_{1,4}{}^{\dagger}} k^0_{2,3}\left(k^{0(2)}_{1,3}k^{0(1)}_{3,1}-k^{0(1)}_{1,3}k^{0(2)}_{3,1}\right)k^0_{4,5}k^{0(1)}_{5,1} + e^{\epsilon^{\dagger(2)}_{3,1}+\epsilon^{\dagger(2)}_{5,1}+\epsilon_{1,4}{}^{\dagger}}\left(k^0_{1,2}k^0_{2,3}k^{0(1)}_{3,1}-k^{0(1)}_{1,3}k^0_{2,1}k^0_{3,2}\right)k^0_{4,5}k^{0(1)}_{5,1} \\
& + e^{\epsilon^{\dagger(1)}_{3,1}+\epsilon^{\dagger(2)}_{3,1}+\epsilon_{4,5}{}^{\dagger}} k^0_{2,1}k^0_{3,2}k^0_{4,1}\left(k^{0(2)}_{1,5}k^{0(1)}_{5,1}-k^{0(1)}_{1,5}k^{0(2)}_{5,1}\right) + e^{\epsilon^{\dagger(1)}_{3,1}+\epsilon^{\dagger(1)(2)}_{3,1}+\epsilon_{1,4}{}^{\dagger}} k^0_{2,1}k^0_{3,2}k^0_{4,5}\left(k^{0(2)}_{1,5}k^{0(1)}_{5,1}-k^{0(1)}_{1,5}k^{0(2)}_{5,1}\right) \\
& + e^{\epsilon^{\dagger(1)}_{5,1}+\epsilon^{\dagger(2)}_{5,1}+\epsilon_{2,3}{}^{\dagger}} k^0_{2,1}\left(k^{0(2)}_{1,3}k^{0(1)}_{3,1}-k^{0(1)}_{1,3}k^{0(2)}_{3,1}\right)k^0_{4,1}k^0_{5,4} + e^{\epsilon^{\dagger(1)}_{5,1}+\epsilon^{\dagger(2)}_{5,1}+\epsilon_{1,2}{}^{\dagger}} k^0_{2,3}\left(k^{0(2)}_{1,3}k^{0(1)}_{3,1}-k^{0(1)}_{1,3}k^{0(2)}_{3,1}\right)k^0_{4,1}k^0_{5,4} \\
& + e^{\epsilon^{\dagger(1)}_{5,1}+\epsilon^{\dagger(2)}_{5,1}+\epsilon^{\dagger(2)}_{3,1}}\left(k^0_{1,2}k^0_{2,3}k^{0(1)}_{3,1}-k^{0(1)}_{1,3}k^0_{2,1}k^0_{3,2}\right)k^0_{4,1}k^0_{5,4} + e^{\epsilon^{\dagger(1)}_{3,1}+\epsilon^{\dagger(2)}_{3,1}+\epsilon^{\dagger(2)}_{5,1}} k^0_{2,1}k^0_{3,2}\left(k^0_{1,4}k^0_{4,5}k^{0(1)}_{5,1}-k^{0(1)}_{1,5}k^0_{4,1}k^0_{5,4}\right)\Bigg] \Bigg/ \\
\Bigg[& e^{\epsilon^{\dagger(1)}_{3,1}+\epsilon_{2,3}{}^{\dagger}+\epsilon_{4,5}{}^{\dagger}} k^0_{2,1}k^0_{4,1}\left(k^{0(2)}_{1,5}k^{0(1)}_{5,1}-k^{0(1)}_{1,5}k^{0(2)}_{5,1}\right)k^{0(2)}_{3,1} + e^{\epsilon^{\dagger(1)}_{3,1}+\epsilon_{1,2}{}^{\dagger}+\epsilon_{4,5}{}^{\dagger}} k^0_{2,3}k^0_{4,1}\left(k^{0(2)}_{1,5}k^{0(1)}_{5,1}-k^{0(1)}_{1,5}k^{0(2)}_{5,1}\right)k^{0(2)}_{3,1} \\
& + e^{\epsilon^{\dagger(1)}_{3,1}+\epsilon_{1,4}{}^{\dagger}+\epsilon_{2,3}{}^{\dagger}} k^0_{2,1}k^0_{4,5}\left(k^{0(2)}_{1,5}k^{0(1)}_{5,1}-k^{0(1)}_{1,5}k^{0(2)}_{5,1}\right)k^{0(2)}_{3,1} + e^{\epsilon^{\dagger(1)}_{3,1}+\epsilon_{1,2}{}^{\dagger}+\epsilon_{1,4}{}^{\dagger}} k^0_{2,3}k^0_{4,5}\left(k^{0(2)}_{1,5}k^{0(1)}_{5,1}-k^{0(1)}_{1,5}k^{0(2)}_{5,1}\right)k^{0(2)}_{3,1} \\
& - e^{\epsilon^{\dagger(1)}_{3,1}+\epsilon^{\dagger(1)}_{5,1}+\epsilon_{2,3}{}^{\dagger}} k^0_{2,1}\left(k^0_{1,4}k^0_{4,5}k^{0(2)}_{5,1}-k^{0(2)}_{1,5}k^0_{4,1}k^0_{5,4}\right)k^{0(2)}_{3,1} - e^{\epsilon^{\dagger(1)}_{3,1}+\epsilon^{\dagger(1)}_{5,1}+\epsilon_{1,2}{}^{\dagger}} k^0_{2,3}\left(k^0_{1,4}k^0_{4,5}k^{0(2)}_{5,1}-k^{0(2)}_{1,5}k^0_{4,1}k^0_{5,4}\right)k^{0(2)}_{3,1} \\
& + e^{\epsilon^{\dagger(2)}_{3,1}+\epsilon_{2,3}{}^{\dagger}+\epsilon_{4,5}{}^{\dagger}} k^0_{2,1}k^0_{4,1}\left(k^{0(2)}_{1,5}k^{0(1)}_{5,1}-k^{0(1)}_{1,5}k^{0(2)}_{5,1}\right)k^{0(1)}_{3,1} + e^{\epsilon^{\dagger(2)}_{3,1}+\epsilon_{1,2}{}^{\dagger}+\epsilon_{4,5}{}^{\dagger}} k^0_{2,3}k^0_{4,1}\left(k^{0(2)}_{1,5}k^{0(1)}_{5,1}-k^{0(1)}_{1,5}k^{0(2)}_{5,1}\right)k^{0(1)}_{3,1} \\
& + e^{\epsilon^{\dagger(2)}_{3,1}+\epsilon_{1,4}{}^{\dagger}+\epsilon_{2,3}{}^{\dagger}} k^0_{2,1}k^0_{4,5}\left(k^{0(2)}_{1,5}k^{0(1)}_{5,1}-k^{0(1)}_{1,5}k^{0(2)}_{5,1}\right)k^{0(1)}_{3,1} + e^{\epsilon^{\dagger(2)}_{3,1}+\epsilon_{1,2}{}^{\dagger}+\epsilon_{1,4}{}^{\dagger}} k^0_{2,3}k^0_{4,5}\left(k^{0(2)}_{1,5}k^{0(1)}_{5,1}-k^{0(1)}_{1,5}k^{0(2)}_{5,1}\right)k^{0(1)}_{3,1} \\
& - e^{\epsilon^{\dagger(1)}_{5,1}+\epsilon^{\dagger(2)}_{3,1}+\epsilon_{2,3}{}^{\dagger}} k^0_{2,1}\left(k^0_{1,4}k^0_{4,5}k^{0(2)}_{5,1}-k^{0(2)}_{1,5}k^0_{4,1}k^0_{5,4}\right)k^{0(1)}_{3,1} - e^{\epsilon^{\dagger(1)}_{5,1}+\epsilon^{\dagger(2)}_{3,1}+\epsilon_{1,2}{}^{\dagger}} k^0_{2,3}\left(k^0_{1,4}k^0_{4,5}k^{0(2)}_{5,1}-k^{0(2)}_{1,5}k^0_{4,1}k^0_{5,4}\right)k^{0(1)}_{3,1} \\
& + e^{\epsilon^{\dagger(1)}_{5,1}+\epsilon_{2,3}{}^{\dagger}+\epsilon_{4,5}{}^{\dagger}} k^0_{2,1}\left(k^{0(2)}_{1,3}k^{0(1)}_{3,1}-k^{0(1)}_{1,3}k^{0(2)}_{3,1}\right)k^0_{4,1}k^{0(2)}_{5,1} + e^{\epsilon^{\dagger(1)}_{5,1}+\epsilon_{1,2}{}^{\dagger}+\epsilon_{4,5}{}^{\dagger}} k^0_{2,3}\left(k^{0(2)}_{1,3}k^{0(1)}_{3,1}-k^{0(1)}_{1,3}k^{0(2)}_{3,1}\right)k^0_{4,1}k^{0(2)}_{5,1} \\
& - e^{\epsilon^{\dagger(1)}_{3,1}+\epsilon^{\dagger(1)}_{5,1}+\epsilon_{4,5}{}^{\dagger}}\left(k^0_{1,2}k^0_{2,3}k^{0(2)}_{3,1}-k^{0(2)}_{1,3}k^0_{2,1}k^0_{3,2}\right)k^0_{4,1}k^{0(2)}_{5,1} + e^{\epsilon^{\dagger(2)}_{5,1}+\epsilon_{1,4}{}^{\dagger}+\epsilon_{2,3}{}^{\dagger}} k^0_{2,1}\left(k^{0(2)}_{1,3}k^{0(1)}_{3,1}-k^{0(1)}_{1,3}k^{0(2)}_{3,1}\right)k^0_{4,5}k^{0(2)}_{5,1} \\
& + e^{\epsilon^{\dagger(2)}_{5,1}+\epsilon_{1,2}{}^{\dagger}+\epsilon_{1,4}{}^{\dagger}} k^0_{2,3}\left(k^{0(2)}_{1,3}k^{0(1)}_{3,1}-k^{0(1)}_{1,3}k^{0(2)}_{3,1}\right)k^0_{4,5}k^{0(2)}_{5,1} - e^{\epsilon^{\dagger(1)}_{3,1}+\epsilon^{\dagger(1)}_{5,1}+\epsilon_{1,4}{}^{\dagger}}\left(k^0_{1,2}k^0_{2,3}k^{0(2)}_{3,1}-k^{0(2)}_{1,3}k^0_{2,1}k^0_{3,2}\right)k^0_{4,5}k^{0(2)}_{5,1} \\
& + e^{\epsilon^{\dagger(2)}_{5,1}+\epsilon_{2,3}{}^{\dagger}+\epsilon_{4,5}{}^{\dagger}} k^0_{2,1}\left(k^{0(2)}_{1,3}k^{0(1)}_{3,1}-k^{0(1)}_{1,3}k^{0(2)}_{3,1}\right)k^0_{4,1}k^{0(1)}_{5,1} + e^{\epsilon^{\dagger(2)}_{5,1}+\epsilon_{1,2}{}^{\dagger}+\epsilon_{4,5}{}^{\dagger}} k^0_{2,3}\left(k^{0(2)}_{1,3}k^{0(1)}_{3,1}-k^{0(1)}_{1,3}k^{0(2)}_{3,1}\right)k^0_{4,1}k^{0(1)}_{5,1} \\
& - e^{\epsilon^{\dagger(1)}_{3,1}+\epsilon^{\dagger(2)}_{5,1}+\epsilon_{4,5}{}^{\dagger}}\left(k^0_{1,2}k^0_{2,3}k^{0(2)}_{3,1}-k^{0(2)}_{1,3}k^0_{2,1}k^0_{3,2}\right)k^0_{4,1}k^{0(1)}_{5,1} + e^{\epsilon^{\dagger(2)}_{5,1}+\epsilon_{1,4}{}^{\dagger}+\epsilon_{2,3}{}^{\dagger}} k^0_{2,1}\left(k^{0(2)}_{1,3}k^{0(1)}_{3,1}-k^{0(1)}_{1,3}k^{0(2)}_{3,1}\right)k^0_{4,5}k^{0(1)}_{5,1} \\
& + e^{\epsilon^{\dagger(2)}_{5,1}+\epsilon_{1,2}{}^{\dagger}+\epsilon_{1,4}{}^{\dagger}} k^0_{2,3}\left(k^{0(2)}_{1,3}k^{0(1)}_{3,1}-k^{0(1)}_{1,3}k^{0(2)}_{3,1}\right)k^0_{4,5}k^{0(1)}_{5,1} - e^{\epsilon^{\dagger(1)}_{3,1}+\epsilon^{\dagger(2)}_{5,1}+\epsilon_{1,4}{}^{\dagger}}\left(k^0_{1,2}k^0_{2,3}k^{0(2)}_{3,1}-k^{0(2)}_{1,3}k^0_{2,1}k^0_{3,2}\right)k^0_{4,5}k^{0(1)}_{5,1} \\
& + e^{\epsilon^{\dagger(1)}_{3,1}+\epsilon^{\dagger(2)}_{3,1}+\epsilon_{4,5}{}^{\dagger}} k^0_{2,1}k^0_{3,2}k^0_{4,1}\left(k^{0(2)}_{1,5}k^{0(1)}_{5,1}-k^{0(1)}_{1,5}k^{0(2)}_{5,1}\right) + e^{\epsilon^{\dagger(1)}_{3,1}+\epsilon^{\dagger(2)}_{3,1}+\epsilon_{1,4}{}^{\dagger}} k^0_{2,1}k^0_{3,2}k^0_{4,5}\left(k^{0(2)}_{1,5}k^{0(1)}_{5,1}-k^{0(1)}_{1,5}k^{0(2)}_{5,1}\right) \\
& + e^{\epsilon^{\dagger(1)}_{5,1}+\epsilon^{\dagger(2)}_{5,1}+\epsilon_{2,3}{}^{\dagger}} k^0_{2,1}\left(k^{0(2)}_{1,3}k^{0(1)}_{3,1}-k^{0(1)}_{1,3}k^{0(2)}_{3,1}\right)k^0_{4,1}k^0_{5,4} + e^{\epsilon^{\dagger(1)}_{5,1}+\epsilon^{\dagger(2)}_{5,1}+\epsilon_{1,2}{}^{\dagger}} k^0_{2,3}\left(k^{0(2)}_{1,3}k^{0(1)}_{3,1}-k^{0(1)}_{1,3}k^{0(2)}_{3,1}\right)k^0_{4,1}k^0_{5,4} \\
& - e^{\epsilon^{\dagger(1)}_{3,1}+\epsilon^{\dagger(1)}_{5,1}+\epsilon^{\dagger(2)}_{5,1}}\left(k^0_{1,2}k^0_{2,3}k^{0(2)}_{3,1}-k^{0(2)}_{1,3}k^0_{2,1}k^0_{3,2}\right)k^0_{4,1}k^0_{5,4} - e^{\epsilon^{\dagger(1)}_{3,1}+\epsilon^{\dagger(2)}_{3,1}+\epsilon^{\dagger(1)}_{5,1}} k^0_{2,1}k^0_{3,2}\left(k^0_{1,4}k^0_{4,5}k^{0(2)}_{5,1}-k^{0(2)}_{1,5}k^0_{4,1}k^0_{5,4}\right)\Bigg] \\
& + \ln\left(\frac{k^0_{1,2}k^0_{2,3}k^{0(2)}_{3,1}}{k^{0(2)}_{1,3}k^0_{2,1}k^0_{3,2}}\right) \Bigg/ \ln\left(\frac{k^0_{1,2}k^0_{2,3}k^{0(1)}_{3,1}}{k^{0(1)}_{1,3}k^0_{2,1}k^0_{3,2}}\right). \qquad \text{(S29)}
\end{aligned}
$$

The invariance of the error rate J_W/J_R and the normalized energy dissipation σ_N is a consequence of Eq. (11) in the main text.

Myosin-V Network

Kinetic Parameters: Myosin-V Motor Protein

Table. S3 lists the kinetic parameters for the mechanochemical network that describes the motion of the myosin-V motor protein as it walks on actin cytoskeleton filaments (see Fig. $4A - D$ in the main text). This biological process is powered by energy from ATP hydrolysis, which enables the myosin-V to take one ~ 36 nm step forward an actin filament while simultaneously carrying a load that exerts an opposing force F_{external} on the motor protein[4,15–19]. This kinetic model for myosin-V illustrates that the motor protein can move one step forward or backward on the actin track (via states 1-5) during a main stepping cycle or it can remain at the same position on the track during a futile cycle (via states 2, 3, 4, and 6).

Table S3: Rate Constants $k_{i,j}$ for the Myosin-V Motor Protein

System Parameters	Myosin-V
$k_{1,2}$	1×10^5
$k_{2,1}$	0.49
$k_{2,3}$	4.6×10^3
$k_{3,2}$	6.4×10^4
$k_{3,4}$	3×10^3
$k_{4,3}$	4.64
$k_{4,5}$	15.2
$k_{5,4}$	3.35
$k_{5,1}$	302.8
$k_{1,5}$	0.62
$k_{4,6}$	6.9×10^{-2}
$k_{6,4}$	1.5×10^{-2}
$k_{6,2}$	302.8
$k_{2,6}$	1.27×10^{-6}

The values of $k_{i,j}$ (in units of s^{-1}) for this kinetic model were obtained from energetic data and kinetic parameters reported in Ref. 17. The [ATP]=[P_i]=1 mM and [ADP]=10 μM at physiological conditions, and the motor protein is carrying a load of $F_{\text{external}} = 0.1$ pN. The chemical potential differences at these physiological conditions for the futile and the main cycles respectively are $\Delta\mu_{\text{futile}} \sim 25\ k_BT$ and $\Delta\mu_{\text{main}} \sim 24\ k_BT$.

Analytic Expressions: Ratio of the Backward- to Forward-Stepping Fluxes and Normalized Energy Dissipation

The analytic expression for the ratio of the backward-stepping flux J_B to the forward-stepping flux J_F of the myosin-V motor protein written in a generalized Kramer's form is:

$$
\begin{aligned}
\frac{J_B}{J_F} = \Bigg[& k^0_{2,1}\left(e^{\epsilon_{4,5}{}^\dagger+\epsilon_{4,6}{}^\dagger}k^0_{1,2}k^0_{3,2}k^0_{4,3}k^0_{5,1}k^0_{6,2} + e^{\epsilon_{3,4}{}^\dagger+\epsilon_{4,6}{}^\dagger}k^0_{1,2}k^0_{3,2}k^0_{4,5}k^0_{5,1}k^0_{6,2} + e^{\epsilon_{2,3}{}^\dagger+\epsilon_{4,6}{}^\dagger}k^0_{1,2}k^0_{3,4}k^0_{4,5}k^0_{5,1}k^0_{6,2}\right) \\
& + k^0_{2,1}\left(e^{\epsilon_{3,4}{}^\dagger+\epsilon_{4,5}{}^\dagger}k^0_{1,2}k^0_{3,2}k^0_{4,6}k^0_{5,1}k^0_{6,2} + e^{\epsilon_{2,3}{}^\dagger+\epsilon_{4,5}{}^\dagger}k^0_{1,2}k^0_{3,4}k^0_{4,6}k^0_{5,1}k^0_{6,2} + e^{\epsilon_{4,6}{}^\dagger+\epsilon_{5,1}{}^\dagger}k^0_{1,2}k^0_{3,2}k^0_{4,3}k^0_{5,4}k^0_{6,2}\right) \\
& + k^0_{2,1}\left(e^{\epsilon_{1,2}{}^\dagger+\epsilon_{4,6}{}^\dagger}k^0_{1,5}k^0_{3,2}k^0_{4,3}k^0_{5,4}k^0_{6,2} + e^{\epsilon_{3,4}{}^\dagger+\epsilon_{5,1}{}^\dagger}k^0_{1,2}k^0_{3,2}k^0_{4,6}k^0_{5,4}k^0_{6,2} + e^{\epsilon_{1,2}{}^\dagger+\epsilon_{3,4}{}^\dagger}k^0_{1,5}k^0_{3,2}k^0_{4,6}k^0_{5,4}k^0_{6,2}\right) \\
& + k^0_{2,1}\left(e^{\epsilon_{2,3}{}^\dagger+\epsilon_{5,1}{}^\dagger}k^0_{1,2}k^0_{3,4}k^0_{4,6}k^0_{5,4}k^0_{6,2} + e^{\epsilon_{1,2}{}^\dagger+\epsilon_{2,3}{}^\dagger}k^0_{1,5}k^0_{3,4}k^0_{4,6}k^0_{5,4}k^0_{6,2} + e^{\epsilon_{4,5}{}^\dagger+\epsilon_{6,2}{}^\dagger}k^0_{1,2}k^0_{3,2}k^0_{4,3}k^0_{5,1}k^0_{6,4}\right) \\
& + k^0_{2,1}\left(e^{\epsilon_{3,4}{}^\dagger+\epsilon_{6,2}{}^\dagger}k^0_{1,2}k^0_{3,2}k^0_{4,5}k^0_{5,1}k^0_{6,4} + e^{\epsilon_{2,3}{}^\dagger+\epsilon_{6,2}{}^\dagger}k^0_{1,2}k^0_{3,4}k^0_{4,5}k^0_{5,1}k^0_{6,4} + e^{\epsilon_{5,1}{}^\dagger+\epsilon_{6,2}{}^\dagger}k^0_{1,2}k^0_{3,2}k^0_{4,3}k^0_{5,4}k^0_{6,4}\right) \\
& + k^0_{2,1}\left(e^{\epsilon_{1,2}{}^\dagger+\epsilon_{6,2}{}^\dagger}k^0_{1,5}k^0_{3,2}k^0_{4,3}k^0_{5,4}k^0_{6,4}\right)\Bigg] \Bigg/ \\
& \Bigg[k^0_{1,2}\left(e^{\epsilon_{4,5}{}^\dagger+\epsilon_{4,6}{}^\dagger}k^0_{2,1}k^0_{3,2}k^0_{4,3}k^0_{5,1}k^0_{6,2} + e^{\epsilon_{3,4}{}^\dagger+\epsilon_{4,6}{}^\dagger}k^0_{2,1}k^0_{3,2}k^0_{4,5}k^0_{5,1}k^0_{6,2} + e^{\epsilon_{2,3}{}^\dagger+\epsilon_{4,6}{}^\dagger}k^0_{2,1}k^0_{3,4}k^0_{4,5}k^0_{5,1}k^0_{6,2}\right) \\
& + k^0_{1,2}\left(e^{\epsilon_{1,2}{}^\dagger+\epsilon_{4,6}{}^\dagger}k^0_{2,3}k^0_{3,4}k^0_{4,5}k^0_{5,1}k^0_{6,2} + e^{\epsilon_{3,4}{}^\dagger+\epsilon_{4,5}{}^\dagger}k^0_{2,1}k^0_{3,2}k^0_{4,6}k^0_{5,1}k^0_{6,2} + e^{\epsilon_{2,3}{}^\dagger+\epsilon_{4,5}{}^\dagger}k^0_{2,1}k^0_{3,4}k^0_{4,6}k^0_{5,1}k^0_{6,2}\right) \\
& + k^0_{1,2}\left(e^{\epsilon_{4,6}{}^\dagger+\epsilon_{5,1}{}^\dagger}k^0_{2,1}k^0_{3,2}k^0_{4,3}k^0_{5,4}k^0_{6,2} + e^{\epsilon_{3,4}{}^\dagger+\epsilon_{5,1}{}^\dagger}k^0_{2,1}k^0_{3,2}k^0_{4,6}k^0_{5,4}k^0_{6,2} + e^{\epsilon_{2,3}{}^\dagger+\epsilon_{5,1}{}^\dagger}k^0_{2,1}k^0_{3,4}k^0_{4,6}k^0_{5,4}k^0_{6,2}\right) \\
& + k^0_{1,2}\left(e^{\epsilon_{4,5}{}^\dagger+\epsilon_{6,2}{}^\dagger}k^0_{2,1}k^0_{3,2}k^0_{4,3}k^0_{5,1}k^0_{6,4} + e^{\epsilon_{3,4}{}^\dagger+\epsilon_{6,2}{}^\dagger}k^0_{2,1}k^0_{3,2}k^0_{4,5}k^0_{5,1}k^0_{6,4} + e^{\epsilon_{1,2}{}^\dagger+\epsilon_{3,4}{}^\dagger}k^0_{2,6}k^0_{3,2}k^0_{4,5}k^0_{5,1}k^0_{6,4}\right) \\
& + k^0_{1,2}\left(e^{\epsilon_{2,3}{}^\dagger+\epsilon_{6,2}{}^\dagger}k^0_{2,1}k^0_{3,4}k^0_{4,5}k^0_{5,1}k^0_{6,4} + e^{\epsilon_{1,2}{}^\dagger+\epsilon_{6,2}{}^\dagger}k^0_{2,3}k^0_{3,4}k^0_{4,5}k^0_{5,1}k^0_{6,4} + e^{\epsilon_{1,2}{}^\dagger+\epsilon_{2,3}{}^\dagger}k^0_{2,6}k^0_{3,4}k^0_{4,5}k^0_{5,1}k^0_{6,4}\right) \\
& + k^0_{1,2}\left(e^{\epsilon_{5,1}{}^\dagger+\epsilon_{6,2}{}^\dagger}k^0_{2,1}k^0_{3,2}k^0_{4,3}k^0_{5,4}k^0_{6,4}\right)\Bigg].
\end{aligned}
\tag{S30}
$$

Notably, this ratio does not depend on the energies ϵ_i of any intermediate states and only depends on the transition state energies $\epsilon^\dagger_{i,j}$. As such, this ratio of the fluxes is invariant to the energy perturbations of the intermediate states on the free energy landscape. Moreover, the normalized energy dissipation σ_N (see Eq. (13) in the main text) depends on the ratio of the fluxes for the futile and the main cycles $J_{\text{futile}}/J_{\text{main}}$, and this property is also invariant to the energy perturbations of the intermediate states on the free energy landscape. The following analytic expression for the normalized energy dissipation written in a generalized Kramer's form depends only on the transition state energies $\epsilon^\dagger_{i,j}$:

$$
\begin{aligned}
\sigma_N = \Bigg[& k^0_{1,2}k^0_{5,1}\left(k^0_{2,3}k^0_{3,4}k^0_{4,6}k^0_{6,2} - k^0_{2,6}k^0_{3,2}k^0_{4,3}k^0_{6,4}\right)e^{\epsilon_{4,5}{}^\dagger} + k^0_{1,2}k^0_{5,4}\left(k^0_{2,3}k^0_{3,4}k^0_{4,6}k^0_{6,2} - k^0_{2,6}k^0_{3,2}k^0_{4,3}k^0_{6,4}\right)e^{\epsilon_{5,1}{}^\dagger} \\
& + k^0_{1,5}k^0_{5,4}\left(k^0_{2,3}k^0_{3,4}k^0_{4,6}k^0_{6,2} - k^0_{2,6}k^0_{3,2}k^0_{4,3}k^0_{6,4}\right)e^{\epsilon_{1,2}{}^\dagger} + k^0_{3,2}\left(k^0_{1,5}k^0_{2,1}k^0_{4,6}k^0_{5,4}k^0_{6,2} - k^0_{1,2}k^0_{2,6}k^0_{4,5}k^0_{5,1}k^0_{6,4}\right)e^{\epsilon_{3,4}{}^\dagger} \\
& + k^0_{3,4}\left(k^0_{1,5}k^0_{2,1}k^0_{4,6}k^0_{5,4}k^0_{6,2} - k^0_{1,2}k^0_{2,6}k^0_{4,5}k^0_{5,1}k^0_{6,4}\right)e^{\epsilon_{2,3}{}^\dagger}\Bigg] \Bigg/ \\
& \Bigg[\left(k^0_{1,2}k^0_{2,3}k^0_{3,4}k^0_{4,5}k^0_{5,1} - k^0_{1,5}k^0_{2,1}k^0_{3,2}k^0_{4,3}k^0_{5,4}\right)k^0_{6,2}e^{\epsilon_{4,6}{}^\dagger} + \left(k^0_{1,2}k^0_{2,3}k^0_{3,4}k^0_{4,5}k^0_{5,1} - k^0_{1,5}k^0_{2,1}k^0_{3,2}k^0_{4,3}k^0_{5,4}\right)k^0_{6,4}e^{\epsilon_{6,2}{}^\dagger} \\
& + k^0_{3,4}\left(k^0_{1,2}k^0_{2,6}k^0_{4,5}k^0_{5,1}k^0_{6,4} - k^0_{1,5}k^0_{2,1}k^0_{4,6}k^0_{5,4}k^0_{6,2}\right)e^{\epsilon_{2,3}{}^\dagger} + \left(k^0_{1,2}k^0_{2,6}k^0_{3,2}k^0_{4,5}k^0_{5,1}k^0_{6,4} - k^0_{1,5}k^0_{2,1}k^0_{3,2}k^0_{4,6}k^0_{5,4}k^0_{6,2}\right)e^{\epsilon_{3,4}{}^\dagger}\Bigg] \\
& + \ln\left(\frac{k^0_{1,2}k^0_{2,3}k^0_{3,4}k^0_{4,5}k^0_{5,1}}{k^0_{1,5}k^0_{2,1}k^0_{3,2}k^0_{4,3}k^0_{5,4}}\right) \Bigg/ \ln\left(\frac{k^0_{2,3}k^0_{3,4}k^0_{4,6}k^0_{6,2}}{k^0_{2,6}k^0_{3,2}k^0_{4,3}k^0_{6,4}}\right).
\end{aligned}
\tag{S31}
$$

The invariance of the ratio of the backward- to forward-stepping fluxes J_B/J_F and the normalized energy dissipation σ_N is a consequence Eq. (11) in the main text.

References

[1] J. Gunawardena, "A linear framework for time-scale separation in nonlinear biochemical systems," PloS One **7**, e36321 (2012).
[2] T. L. Hill, *Free Energy Transduction and Biochemical Cycle Kinetics* (Courier Corporation, 2005).
[3] M. E. Tuckerman, *Statistical Mechanics: Theory and Molecular Simulation* (Oxford University Press, 2010).
[4] A. B. Kolomeisky, *Motor Proteins and Molecular Motors* (CRC Press, Taylor and Francis Group: Boca Raton, FL, 2015).
[5] S. W. Englander, L. Mayne, and M. M. Krishna, "Protein folding and misfolding: mechanism and principles," Q. Rev. Biophys. **40**, 1–41 (2007).
[6] M. M. Krishna and S. W. Englander, "A unified mechanism for protein folding: Predetermined pathways with optional errors," Protein Sci. **16**, 449–464 (2007).
[7] O. Bieri, G. Wildegger, A. Bachmann, C. Wagner, and T. Kiefhaber, "A salt-induced kinetic intermediate is on a new parallel pathway of lysozyme folding," Biochemistry **38**, 12460–12470 (1999).
[8] K. B. Gromadski and M. V. Rodnina, "Kinetic determinants of high-fidelity tRNA discrimination on the ribosome," Mol. Cell **13**, 191 (2004).
[9] N. M. Reynolds, B. A. Lazazzera, and M. Ibba, "Cellular mechanisms that control mistranslation," Nat. Rev. Microbiol. **8**, 849 (2010).
[10] H. S. Zaher and R. Green, "Fidelity at the molecular level: lessons from protein synthesis," Cell **136**, 746–762 (2009).
[11] H. S. Zaher and R. Green, "Hyperaccurate and error-prone ribosomes exploit distinct mechanisms during tRNA selection," Mol. Cell **39**, 110–120 (2010).
[12] K. Banerjee, A. B. Kolomeisky, and O. A. Igoshin, "Elucidating interplay of speed and accuracy in biological error correction," Proc. Natl. Acad. Sci. USA **114**, 5183–5188 (2017).
[13] K. Banerjee, A. B. Kolomeisky, and O. A. Igoshin, "Accuracy of substrate selection by enzymes is controlled by kinetic discrimination," J. Phys. Chem. Lett. **8**, 1552–1556 (2017).
[14] J. D. Mallory, A. B. Kolomeisky, and O. A. Igoshin, "Trade-offs between error, speed, noise, and energy dissipation in biological processes with proofreading," J. Phys. Chem. B **123**, 4718–4725 (2019).
[15] M. Enrique, A. L. Wells, S. S. Rosenfeld, E. M. Ostap, and H. L. Sweeney, "The kinetic mechanism of myosin V," Proc. Natl. Acad. Sci. USA **96**, 13726–13731 (1999).
[16] A. B. Kolomeisky and M. E. Fisher, "A simple kinetic model describes the processivity of myosin-V," Biophys. J. **84**, 1642–1650 (2003).
[17] K. I. Skau, R. B. Hoyle, and M. S. Turner, "A kinetic model describing the processivity of myosin-V," Biophys. J. **91**, 2475–2489 (2006).
[18] A. D. Mehta, R. S. Rock, M. Rief, J. A. Spudich, M. S. Mooseker, and R. E. Cheney, "Myosin-V is a processive actin-based motor," Nature **400**, 590 (1999).
[19] A. Mehta, "Myosin learns to walk," J. Cell Sci. **114**, 1981–1998 (2001)